Identification of Important Residues for Modulation of Allosteric Properties of Potato ADP Glucose Pyrophosphorylase

by

Ayşe Bengisu Seferoğlu

A Thesis Submitted to the
Graduate School of Sciences and Engineering
in Partial Fulfillment of the Requirements for
the Degree of

Master of Science
in
Chemical and Biological Engineering

Koç University

August, 2011

Koç University

Graduate School of Sciences and Engineering

This is to certify that I have examined this copy of a master's thesis by

A. Bengisu Seferoğlu

and have found that it is complete and satisfactory in all respects,

and that any and all revisions required by the final

examining committee have been made.

Committee Members:

_____

İ. Halil Kavaklı, Ph. D.(Advisor)

_____

Özlem Keskin, Ph. D.

_____

Gülayşe İnce Dunn, Ph. D.

Date: _____

to my family…

ABSTRACT

ADP glucose pyrophosphorylase (AGPase) is a key regulatory enzyme of bacterial glycogen and plant starch synthesis as it controls carbon flux via its allosteric regulatory behavior. Whereas the bacterial enzyme is composed of a single subunit type, the plant AGPase is a heterotetrameric enzyme ($\alpha_2\beta_2$) with distinct roles for each of the two subunit types. The large subunit (LS) is involved mainly in allosteric regulation through its interaction with the catalytic small subunit (SS). Previously, critical amino acids of potato (*Solanum tuberosum L.*) LS that interact with SS in the native heterotetramer structure were identified both computationally and experimentally. In this study, we aimed to improve the heterotetrameric assembly of potato AGPase and to detect residues located on the interface involving the allosteric regulation of the enzyme with a reverse genetics approach. A mutant, $\alpha_2\beta_2$ formation deficient, large subunit of potato AGPase named LS_{R88A} was subjected to random mutagenesis using error prone PCR and screened for the capacity to form an enzyme restoring glycogen production in $glgC^-$ *Escherichia coli*, AGPase activity deficient, containing wild type SS by assessing iodine staining. Fifteen suppressor mutants were identified and sequence analysis of these mutants revealed that mutations are mainly clustered at subunit interface and nearby the subunit interface. Subsequently, R88A mutation was reversed with site directed mutagenesis to see the effect of these mutations in the absence of R88A mutation. Kinetic characterization showed that two random mutants, named RM2 and RM10, exhibit altered allosteric properties than the wild type. These results indicate that interfaces between the large and small subunits are significant for the allosteric properties of the AGPase. Obtaining stable and up-regulated AGPase variants will enable us to use these mutants to increase the starch yield in crop plants.

ÖZET

ADP-glikoz pirofosforilaz (AGPaz), allosterik enzim olma özelliğiyle karbon akışını kontrol eden, bakterilerde glikojen; bitkilerde nişasta sentezinde görev alan anahtar bir düzenleyici enzimdir. Bakteri AGPaz'ı tek alt birimden oluşmasına rağmen, bitki AGPaz'ı farklı görevli alt birimler içerip heterotetramer ($\alpha_2\beta_2$) yapıdadır. Büyük alt birim (LS), katalitik olan küçük alt birimle (SS) etkileşerek allosterik düzenlemede görev alır. LS, SS'in katalitik aktivitesini, heterotetramerik enzimin allosterik regülatör cevabını artırarak düzenler. Bitki hücresinde AGPaz'ın kararsız halde bulunduğu bilinmektedir. Önceki çalışmalarda patates AGPaz'ının heterotetramerik modelinde küçük alt birimle etkileşen büyük alt biriminin önemli aminoasitleri hem deneysel hem de hesaplamalı olarak belirlenmiştir. Bu çalışmada amaç ters genetik yaklaşımı ile, patates AGPaz enziminin heterotetramer oluşumunu artırmak ve alt birimlerin birbirleriyle olan etkileşiminin enzimin allosterik düzenlenmesini etkileyip etkilemediğini araştırmaktır. Bu nedenle heterotetramerik enzim oluşturamayan LS_{R88A} mutantı rastgele mutasyona tabi tutulmuş ve SS içeren $glgC^-$ *E.coli* hücresinde (AGPaz akitivitesi olmayan) glikojen üretimini geri kazananların iyot buharı ile boyama yöntemiyle seçilmesi amaçlanmıştır. 15 baskılayıcı mutant seçilmiş ve mutantların sekans analizi mutasyonların bir kısmının alt birim ara yüzünde meydana geldiğini göstermiştir. Bir sonraki aşamada, seçilen mutantlarda R88A mutasyonunun varlığında veya yokluğunda heterotetramer oluşumunun artıp artmadığına bakmak için R88A mutasyonu, bölgeye yönlendirilmiş mutajenez ile geri çevrildi. RM2 ve RM10 mutantlarının kinetik karakterizasyonu bu mutantların yabanıl tip enzime göre farklı allosterik özelliklere sahip olduğunu gösterdi. Bu sonuçlar büyük alt birim ve küçük alt birim arasındaki ara yüzün AGPaz enziminin allosterik özellikleri için önemli olduğunu göstermektedir. Daha karalı ve daha iyi regüle olan AGPaz varyantlarını elde etmek, bu mutantların bitkilerdeki nişasta miktarını artırmak için kullanılmasını sağlayacaktır.

ACKNOWLEDGEMENTS

I would like to express my sincere thanks to my advisor İ. Halil Kavaklı for his supports, advice and most of all his patience. His experience and great knowledge did not only guide me through my graduate study but also inspired me to continue my academic career. It was a great pleasure and honor to be a member of his research group.

I acknowledge the financial support of the Scientific and Technological Research Council of Turkey (TÜBİTAK) during my whole graduate study.

I especially thank İbrahim Barış, Ph.D. and Hande Asımgil, Msc. for teaching the lab techniques and their endless support in my studies.

I would like to give my special thanks to my dear friends Hande Asimgil, Onur Öztaş and Bilal Çakır for their endless help and friendship and good times for these two years. I would also thank Mehmet Tardu and Hande Morgil. I also would like to thank the former lab members Natali Özber, Sibel Kalyoncu and especially Onur Dağlıyan.

I would like to give my special thanks to my housemates Melis Yavuz and Zeynep Ülker who made these two years an enjoyable period of time with their endless support and friendship. Special thanks go again to my dear friend of many years: Anı Akpınar. It would be impossible to finish this degree without your support and lifelong friendship.

Last but not least, I would like to thank my family and Çağıl Erk Demir for their continuous support, patience and endless love during every step of my education.

TABLE OF CONTENTS

LIST OF TABLES

LIST OF FIGURES

NOMENCLATURE

AGPase	ADP glucose pyrophosphorylase
ADPGlc	ADP glucose
BE	Branching enzyme
CFE	Cell free extract
DEAE	Diethylaminoethyl
DTT	Dithiothreitol
GBSS	Granule bound starch synthase
G1P	Glucose 1 phosphate
HRP	Horseradish peroxidase
LB	Luria Bertani
LS	Large subunit
NAD	Nicotinamide adenine dinucleotide
PCR	Polymerase chain reaction
PMSF	Phenylmethanesulfonylfluoride
P_i	Inorganic phosphate
PP_i	Pyrophosphate
SDS-PAGE	Sodium dodecyl sulfate polyacrylamide gel electrophoresis
SS	Small subunit
WT	Wild type
3PGA	3-Phosphoglyceric acid

Chapter 1

INTRODUCTION

Starch is the major storage carbohydrate in plants which is one of the main nutrients of the world's population. Moreover, starch is recently becoming an alternative raw material for industry with its unique properties e.g. binding, bonding and biodegradability. Due to its significance in nutrition, in industry and in bioethanol production, various approaches have been undertaken to engineer starch for enhancing crop quality and yield [1, 2]. One of the most significant attempts to increase starch accumulation have focused on engineering ADP-glucose pyrophosphorylase (AGPase)[1].

A rate limiting step of starch biosynthesis in plants is catalyzed by AGPase, controlling the carbon flux in the α-glucan pathway by converting Glucose-1-phosphate and ATP to ADP-glucose and pyrophosphate. The activity of the AGPase is allosterically regulated by 3PGA and inorganic phosphate by stimulating and inhibiting the activity of enzyme respectively. Plant AGPases are heterotetrameric ($\alpha_2\beta_2$) enzymes composed of two subunits called large subunit (LS) and small subunit (SS). Whereas LS regulates allosteric behaviors of the enzyme, SS is the catalytic subunit[3]. Previously, critical amino acids of potato (*Solanum tuberosum L.*) LS that interact with SS in the native heterotetramer structure were identified both computationally and experimentally [4]. In this study, we aim to see the influence of changing subunit interface residues on the heterotetrameric assembly and allosteric properties of potato AGPase with a reverse genetics and random mutagenesis approach. A mutant which cannot form α2β2, large subunit of potato (*Solanum tuberosum L.*) AGPase named LS_{R88A} was subjected to random mutagenesis using error prone PCR and screened for the capacity to form an enzyme restoring glycogen production in AGPase deficient

(glgC$^-$)*Escherichia coli* 501R, , containing wild type SS by assessing iodine staining. Plasmids were isolated from the colonies that stained with iodine vapor. The natures of mutations were characterized by DNA sequencing. Then, the effects of mutants were assessed by introducing into the wild type LS cDNA by site directed mutagenesis. Mutants were expressed along with wild type cDNA of the potato SS in glg C$^-$ *E.coli*. Both complementation and biochemical characterization indicated that I obtained mutants that displayed change in their allosteric properties.

In Chapter 2, the corresponding work in the literature is demonstrated. This chapter includes the most recent information about synthesis and importance of starch and the structure, function, regulation of AGPase.

Chapter 3 includes materials and methods, and illustrates the details of the generation and characterization of obtained mutant LS variants. Error prone PCR, cloning of mutant library, screening and selection of putative mutants, expression, and partial purification and of putative mutants are explained in this chapter. In the remaining part of this chapter, *in vitro* enzymatic assays and kinetic characterization putative mutants are presented in detail.

Chapter 4 includes the results of this work and discussion is given in the chapter 5. This thesis ends with chapter 6 which includes the future directions and conclusion of the study.

Chapter 2

LITERATURE REVIEW

2.1. Starch Biosynthesis

Starch is the main storage carbohydrate of plants. In higher plants, starch is stored in the form of granules in the amyloplast of storage tissues including seeds and tubers and in a transitory form in the chloroplast of leaves roots and stems. While the transitory starch is required for respiration, maintenance and sucrose synthesis, storage starch is required for growth or for meeting the high demand of carbon for energy requiring processes [2].

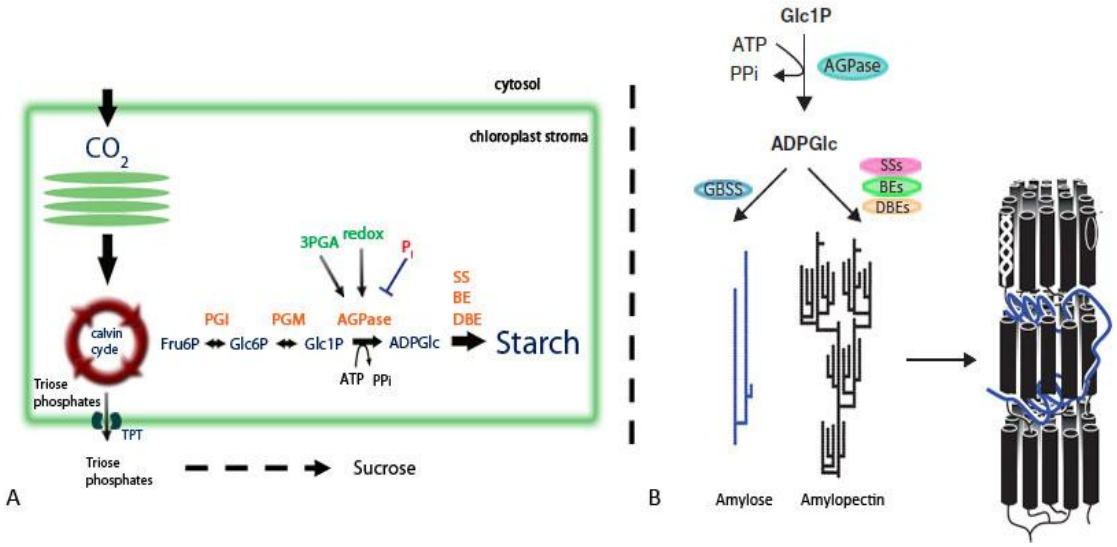

Figure 2.1 Schematic representation of starch synthesis A) Main steps in the starch biosynthetic pathway shown in chloroplast. The carbon flux into starch is controlled by redox activation and allosteric regulation of AGPase. B) Components of starch: moderately branched amylose and highly branched amylopectin molecules and their assembly into starch granule. Amylopectin forms the ordered semi-crystalline arrays with aligned double helices and amylose (blue) forms the unordered structures within the granule. Adapted from [2, 5].

2.1.1. Structure and composition of starch

Starch is the dominant polysaccharide of plants. Since starch does not affect osmotic pressure of the plant cell, sugars produced via photosynthesis are stored in the starch form to supply the energy need of the plant. Starch is the energy supply of germination process and nonphotosynthetic periods. Starch is the fundamental element of cereals, roots and tubers [6]. Transitory starch is produced in leaves and it is smaller than the storage starch of the roots and tubers. The size of the starch depends on the tissue and its diameter changes between 0.1 to 50 μm [7].

Starch granules are composed of amylopectin and amylose polymers. Although those macromolecules resemble each other in the molecular level, the number of glucose residues and the branching levels are different. The linear and few branched amylose molecules have glucose monomers connected with α-1,4 glycosidic bonds. Amylose comprises 30% of the starch granules. Each amylose chain consists of 300 to 3000 glucose monomers. On the other hand, amylopectin is highly branched and α-1,4 glycosidic bonded glucose monomers have α-1,6-glycosidic bonded branching points in each 24^{th} or 30^{th} glucose monomer. The number of glucose monomers change between 3000 and 25000 depending on the plant species. The amylopectin makes up 75% of starch granule [7, 8].

The chemical nature of starch is determined according to glucose chain length and branching level. The chain length is usually determined with amylolytic enzymes such as β-amylase and the branching level is determined by isoamylase and pullanase enzymes. The chemical nature of starch varies among plant species. For example, wheat amylose chain contains 1,9 branching point, whereas this ratio is 7.3 in potato [8].

Granular nature of the storage starch depends on the amylopectin structure in which radially organized amylopectin molecules forms a treelike structure (Figure 2.1). Pairs of adjacent amylopectin chains pack together as double helices and form crystalline layers. Amylose is thought to be present in amorphous zones of the granule [7, 8].

2.2. Starch and Its Industrial Importance

Starch is used not only for nutrition but also for various industrial processes due to its unique properties. It is used in food and beverage industry as thickener and sweetener. Paper and adhesive industry benefit from starch's binding and bonding properties. Since starch is biodegradable, starch based plastics including packaging and catering items are environment friendly alternatives to the petroleum based products. In addition, starch is used for the production of drug capsules in the pharmaceutical sector [1]. Bioethanol production is one of the most interested usage area of starch [9]. All of those benefits and usage areas highlight the importance of biotechnological increase of the starch yield. Various approaches have been attempted to engineer starch for enhancing crop quality and yield. One of those approaches is to control ADP-glucose level by manipulating the enzymes involved in the process. AGPase has been extensively studied, since ADP-glucose is produced by the reaction of AGPase [10, 11].

2.2.1. Starch biosynthesis

There are three main steps of starch biosynthesis (Figure 2.2) [1] in plants.

- Formation of ADPGlc, the glucosyl donor, from Glc 1-P and ATP by a reaction catalyzed by ADPGlc pyrophosphorylase
- Extension of glucose chains with the incorporation of ADPGlc by starch synthases
- Branching and debranching of the glucose chains by starch branching and debranching enzymes

2.3. ADP Glucose Pyrophosphorylase

AGPase catalyzes the first committed step in starch and glycogen biosynthetic pathway in plants and bacteria respectively [12]. In the AGPase catalyzed reaction, G1P and ATP are converted to ADP-Glucose and pyrophosphate. ADP-glucose is then used by starch synthase and starch synthesis continues [1].

Higher plant AGPases are heterotetrameric enzymes ($\alpha_2\beta_2$) composed of two subunit types which evolved from a common ancestral gene [13]. On the other hand, bacterial AGPases are homotetrameric enzymes which are encoded by a single gene. Two distinct subunits of the plant AGPase are called large subunit (LS) and small subunit(SS) with a molecular weight of 51 kDa and 50 kDa respectively [14].

Amyloplasts are the location of leaf and potato tuber AGPases whereas endosperm AGPases are localized mainly in cytosol with a residual activity in the amyloplast [15, 16].

There is 53% sequence identity between the potato tuber AGPase's large and small subunits [17]. Although small subunits of plant AGPases are highly conserved among different plant species, similarity between large subunits is lower [18]. While small subunit is the main catalytic subunit, large subunit has a role in modulating the activity of the AGPase [3, 19, 20]. Small subunit has also regulatory properties [21]. Small subunit of AGPase can form a homotetrameric enzyme which requires higher levels of 3PGA activation and lower levels P_i inhibition. [22]. When homotetrameric SS is fully activated by high concentrations of 3PGA, it shows similar kinetic properties to the wild type heterotetramer and cyanobacterial AGPases [23].

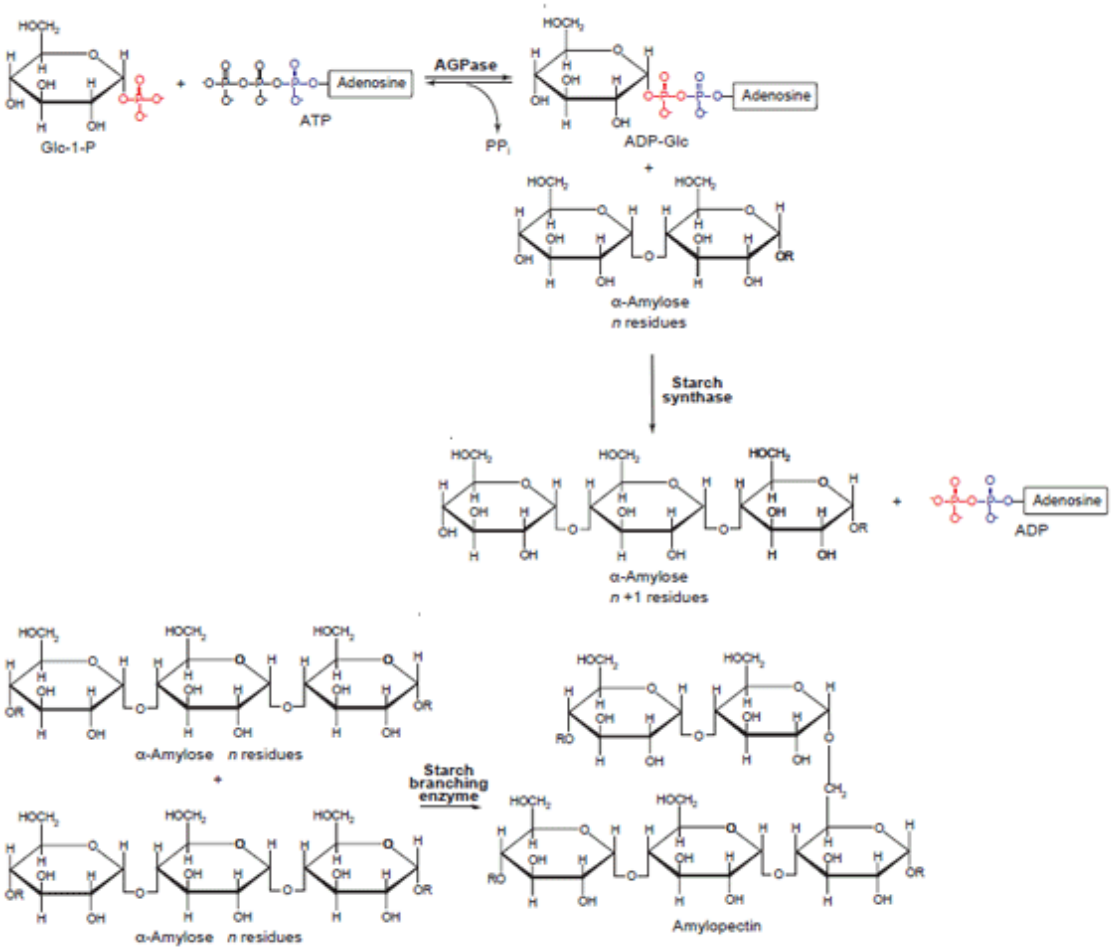

Figure 2.2 The three main enzymes involved in starch biosynthesis and their reactions catalyzed. First step is catalayzed by AGPase, Starch synthase catalyzes second step and starch branching enzyme catalyzes the third step. Adapted from [1]

The reaction catalyzed by AGPase requires the divalent cation, Mg^{++}. Reaction proceeds mainly in the ADP-Glucose synthesis direction although it is freely reversible reaction in vitro [14, 24]. Enteric bacteria AGPase are allosterically regulated by fructose-1,6-bisphosphate and AMP as activator and inhibitor respectively, whereas plant AGPase are activated by 3PGA and inhibited by orthophosphate [14, 24]. The ratio of 3PGA/P_i fluctuates according to diurnal cycling of photosynthesis. Therefore, 3PGA/P_i ratio not only regulates the activity of leaf AGPases, but also regulates carbon

flow into starch [25]. Labeling studies revealed that key lysine residues of both SS and LS have a role in allosteric regulation of the AGPase [26]. Studies showed large subunit has multiple labeling pattern which highlights the allosteric regulation function of the LS [27]. In addition, mutagenesis and reverse genetic studies identified some up-regulated mutant large subunits which have more sensitive and resistant phenotype to 3PGA and P_i respectively [28, 29]. Directed evolution studies of small subunit showed that small subunit exhibits plasticity in its allosteric effector sites when subjected to few point mutations and recombination [30]. Recently, a maize/potato chimeric AGPase was reported to have favorable kinetic and allosteric behaviors. This chimera includes the first 198 amino acids of SS of the maize endosperm and last 277 amino acids of SS potato tuber enzyme [31].

The activity of AGPase is also under control of the redox regulation. A disulfide bond forms between Cys residues of SS when LS and SS coexpressed in *E.coli*. DTT or thioredoxin treatments break the bond and increase the activity of the enzyme [32]. Mutation in the Cys residue, responsible for the disulfide bond created a less heat stable enzyme and a nonresponsive enzyme to DTT [33]. It was shown that potato tuber also has the same process [34]. This activation in planta indicates a new regulation system in which incoming Suc is directed to synthesis of the storage starch [34]. In addition, starch synthesis in leaves is activated by light directly via posttranscriptional redox regulation [35].

Although SS is the main catalytic subunit, there are some studies emphasizing the catalytic role of the LS. The catalytic property of potato LS is resurrected by incorporation of Arg44 and Lys54 which are homolog residues in the SS. Expressing this double mutant with a noncatalytic mutant SS (SS_{D145N}), exhibited catalytic behavior. According to this result, LS recovered its ancestral catalytic ability [36]. In another study, via leucine-scaning mutagenesis, whereas the replacement of $P52_{LS}$ formed a down-regulated enzyme, $P56_{LS}$ formed an up-regulated AGPase. It was also shown that $P44_{LS}$ is significant for catalytic activity, substrate affinity and responses to effectors. In addition LS was labeled by 8-azido-ATP, a substrate analog, which

indicates the catalytic role of the LS. According to the hypothesis, LS binds both effectors and substrates and creates the synergy between the two subunits in the heterotetramer with its pseudo-catalytic properties [37]. Kuhn et al. indicates that since there is fewer SS isoforms than LS isoforms, SS is under the pressure of being and remaining catalytic. Recently, a similar double mutant LS study in *Ostreococcus tauri* AGPase also indicated the ancestral catalytic property of LS [38]. Phylogenetic analysis also agrees with LS is evolved from a catalytic ancestor. Large subunit has higher evolutionary rate than small subunit and so large subunit have gone through more duplication events [39].

2.3.2. Structure of AGPase

The crystal structure of homotetrameric SS potato tuber AGPase was solved in its inhibitor bound and substrate bound states as seen in Figure 2.3 [40]. According to this structure catalytic N-terminus is comprised of mostly parallel but mixed seven stranded β sheets covered by α helices. There is strong hydrophobic interaction between the catalytic domain with the C- terminal β helix domain which are connected by a 20 amino acid long loop. This loop carries the interacting residues with another subunit. Although the subunits are identical in this crystal structure they showed different affinities to ATP and ADPGlc. However, interaction between the allosteric regulatory sites and the active site is still unknown due to the structure being in the inhibited state. According to the hypothesis there is an interaction between the allosteric sites and N-, C-terminal domains of the potato tuber enzyme [40].

Determination of the crystal structure of the heterotetrameric AGPase in its active state will elucidate the exact mechanism of enzyme catalysis and regulation. By that time, information about structure-function relationship of AGPase, its catalytic and regulatory mechanisms will come from experimental and computational studies.

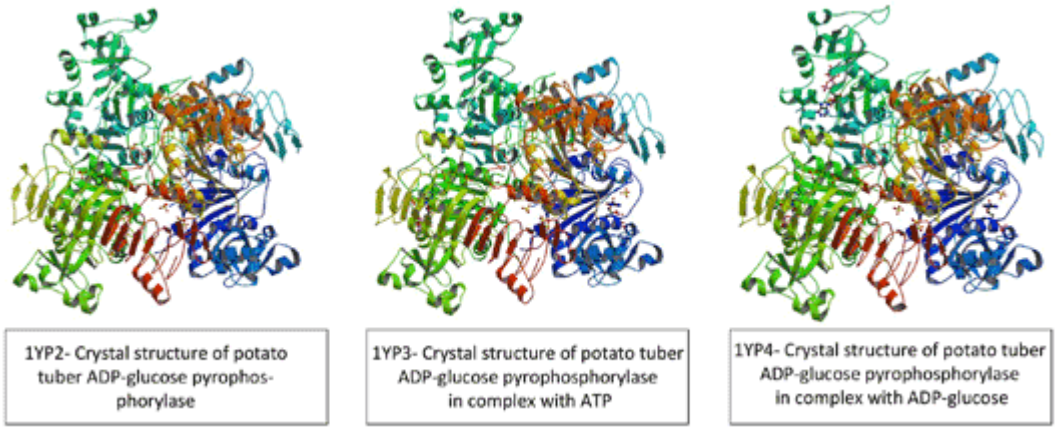

Figure 2.3 Crystal structure of homotetrameric potato tuber AGPase, in its inhibited and substrate and inhibitor bound states. Adapted from [40]

Recent data for structure of AGPase comes from study of *Agrobacterium tumefaciens*' homotetrameric AGPase [41]. The enzyme is crystallized in its sulfate-inhibited form. According to this study, AGPase of *A. tumefacines* is composed of an N-terminal αβα sandwich domain and C-terminal parallel β- helix. Both N- and C-terminal have regulatory binding sites [41].

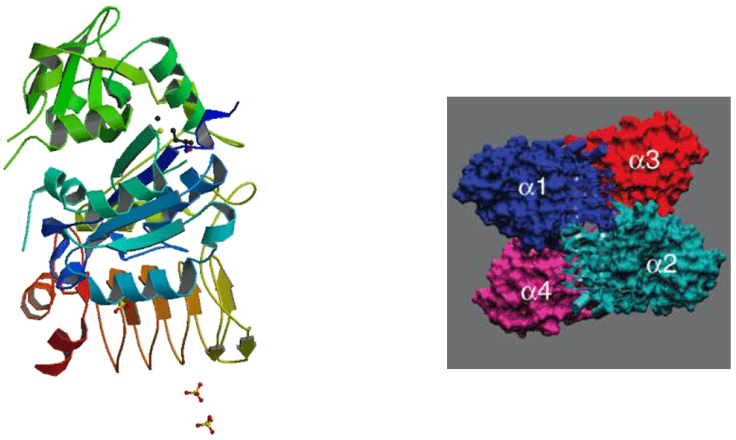

Crystal Structure of AGPase from *Agrobacterium tumefaciens*

The tetramer of *A. tumefaciens* AGPase found in the crystal lattice

Figure 2.4 Crystal structure of Agrobacterium tumefaciens homotetrameric AGPase in its sulfate-inhibited form [41]

2.3.3. Subunit Interaction of AGPase

Information about subunit interaction of AGPase comes from random and site directed mutagenesis and yeast-two hybrid data. Structure-function roles of plant AGPase subunits analyzed by screening randomly mutagenized the cDNA of both subunit by the ability to complementing the mutations in the bacterial AGPase system [42]. Previously, specific regions of both LS and SS were found critical for subunit association and enzyme stability. In the study of Lauglin et al. [43] 19 amino acid segment of C-terminus of both subunits was shown to have a role in subunit association and heterotetrameric enzyme formation. In addition, in the chimeric maize/potato small subunits Cross et al. [44] found a critical polymorphic motif for subunit interaction They revealed a 55 amino acid region between the residues 322-376 in the small subunit interacting directly with the large subunit, effecting enzyme stability. Tuncel et

al.[45] modeled the heterotetrameric potato AGPase structure by homology modeling based on the crystal structure of SS homotetramer (Figure 2.5). Computational and experimental results concluded that most favorable heterotetrameric AGPase is formed by longitudinal and lateral interactions (D2 and D5) of LS and SS [45]. Moreover, they revealed the important residues mediating the interactions between LS and SS for potato AGPase by both computational and experimental techniques. Among energetically most favorable dimers critical amino acid residues for the longitudinal and lateral interaction between subunits were identified. R88 of LS is designated as one of the significant residues for the longitudinal LS-SS interaction. Mutating Arg_{88} to Ala resulted in a heterotetramer formation deficient LS [4].

Important residues of large subunit controlling enzyme properties were identified recently by site-directed mutagenesis studies of conserved large subunit residues. Results indicate the significance of subunit interfaces between LS and SS for the allosteric properties of the enzyme [46].

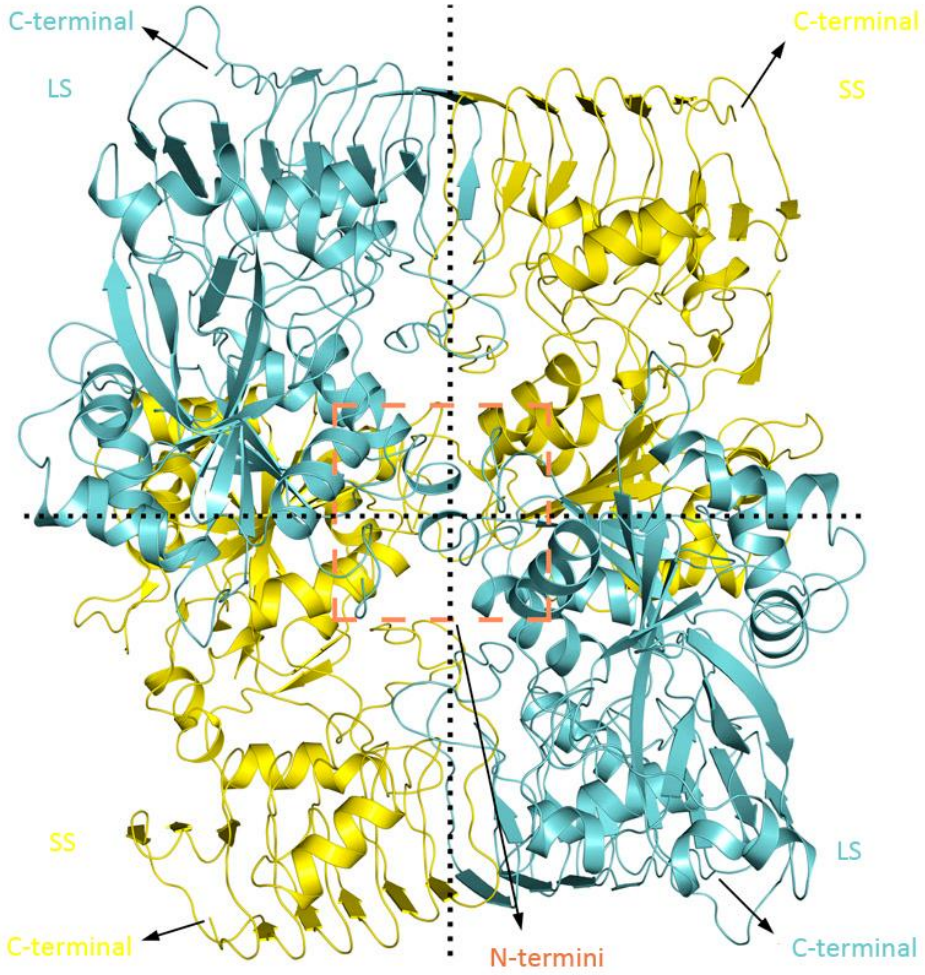

Figure 2.5 Modeled structure of heterotetrameric potato AGPase. LS is represented in cyan and SS represented in yellow. Snapshot shown in red square includes highly conserved residues in the LS-SS interface. Adapted from [45].

2.3.4. The Role of the AGPase in the Regulation of Starch Synthesis

There are ample evidence showing that AGPase is catalyzing the committed step in starch biosynthesis. Starch content deficient mutants (shrunken-2 and brittle-2) were isolated in maize endosperm [47, 48]. In addition, in potato, expression of AGPase was inhibited by introducing a chimeric gene encoding antisense RNA which resulted in abolition of starch formation in tubers [49]. Moreover, expression of a mutated *E.coli* AGPase in potato led to an increase in the starch content of the tubers by 30-60% [11]. Increase of the starch content by transformation of plant with modified AGPase is a significant biotechnological advance and makes possible to increase crop yield.

Obtaining allosteric up-regulated mutants by mutagenesis studies which show higher affinity to the activator and increased resistance to the inhibitor indicates that these kinds of strategies are valid for developing novel variants of the enzyme. Another approach to enhancing properties of AGPase would be to modify subunit interaction of the enzyme due to its tetrameric nature [1]. Small subunit is found as a mixture of monomers and dimers in growing potato tubers. Complete dimerization leads to the inactivation of the enzyme in detached tubers. Dimerization occurs due to the disulfide bond formation between Cys82 residues of the SS [34]. Enhancing the interaction between SS and LS monomers may partially inhibit dimerization of the SSs and inactivation of the enzyme. In addition, improving the heat stability of enzyme and producing chimeric AGPase with improved properties are some of the example approaches as stated in the previous sections [1].

The more we understand the nature of AGPase, the better approaches will be taken to engineer AGPase for increasing starch yield in crop plants.

2.4. Starch Synthase

Starch synthase catalyzes α-1,4 glycosidic bond formation in glucose chain by using ADP-glucose molecules. Five gene classes encode higher plant starch synthases named granule bound starch synthase, starch synthase I, II, III and IV (SSI, SSII, SSIII, SSIV). GBSS synthesizes amylose molecules [12, 50]. The other isoforms of SS produce amylopectin chains. According to the studies of mutant and transgenic plants having deficient SS isoforms SSI elongates short, SSII elongates medium and SSIII elongates long chains of amylopectin [51].

Transgenic plant studies revealed that changes in the enzyme activity also affects the structure of starch [52, 53]. This led to the idea of manipulation of starch structure to diversify its usage in the industry. For example mutant forms of many cereal and legume families were obtained containing only amylopectin or very high amounts of amylose [54]. In addition first transgenic potato and cassava were obtained with no amylose content by downregulating the GBSS [55, 56].

2.5. Branching and Debranching Enzymes

Branching of the amylopectin molecules is catalyzed by the branching enzyme via α-1,6 linkages [1, 57]. Branching process simultaneously occurs with elongation process [57]. Branching enzymes have two classes named class I and class II. Class I enzymes transfer longer chains than class II enzymes [51].

The structure of amylopectin is also determined by debranching enzymes which cleaves branching points. Isoamylase and limitdextrinase are two types of debranching enzymes [58]. Mutant or transgenic plants lacking isoamylase replaced their granular starch with water soluble phytoglycogens. Highly branched structure of phytoglycogens prevents the ordered structure of starch. Multiple mutants lacking all debranching

enzyme activity proved that debranching enzyme activity is definitely required for starch synthesis [59].

Chapter 3

MATERIALS AND METHODS

3.1. Preparing Mutant Library through LS_{R88A}

Mutant library was prepared by random mutagenesis through the LS carrying the mutation R88A. R88A mutation was previously shown to be defective in heterotetrameric functional AGPase formation [4]. It was necessary to get sufficient number of transformants for identifying variants exhibiting glycogen synthesis. An efficient library preparation requires an optimized cloning to obtain high number of transformants and less background. For this reason materials and conditions e.g. competent cells and restriction enzymes need to be suitable and efficient. In other words, cloning of the recombinant plasmids should have been efficient in which background transformants should have been few and conditions were well prepared.

3.1.2. Preparation of Chemically Competent DH5α and Transformation

A single colony of DH5α was inoculated to 5 ml LB. 5 ml o/n grown culture was then inoculated into 500 ml LB and when the OD_{600} of the culture reaches ~0.3-0.4 culture was put on ice until it gets cold. Then culture was transferred to pre-chilled centrifuge tubes. After 10 min centrifugation at 5000 rpm, 4^{o}C pellet was resuspended in 250 ml ice cold $CaCl_2$ solution, centrifuged at 5000 rpm and supernatant was discarded. This washing step was repeated at least two more times with 50 ml and 10 ml $CaCl_2$ solution. Finally pellet was resuspended in 1 ml ice cold $CaCl_2$ solution and cells were dispensed in 100 µl aliquots into prechilled microfuge tubes. Then aliquots of competent cells were frozen in liquid nitrogen and stored at -80^{o}C.

Transformation was performed via heat shock. First, cells and the plasmid were incubated on ice for 10 min, then subjected to 42^{o}C for 90 sec and put on ice immediately. 900 µl LB was added and incubated for 45 to 60 min on 37^{o}C shaker. Then cells were plated on LB medium containing appropriate antibiotics.

3.1.3. Preparation of Electrocompetent glgC^{-} and Transformation

2 ml of a fresh overnight culture was subcultured into 200 ml LB in a 500 ml flask. Cells were grown on 37^{o}C shaker to midlog phase. Cells were centrifuged at 6000 rpm for 10 min at 4^{o}C and resulting pellets were resuspended in 200 ml cold sterile dH_2O. Cells were recentrifuged. Cells were resuspended in 5 ml cold sterile 10% glycerol and centrifuged at 10000 rpm at 4^{o}C for 5 min. Resulting pellet was then resuspended in 1 ml cold sterile glycerol, 40 µl aliquots of the cell suspension were frozen in liquid nitrogen and stored at -80^{o}C.

50 - 100 ng of DNA was added to 40 µl electrocompetent cells, mixed gently and placed pn ice for 1-2 min. Sample was transferred to precooled electroporation cuvette (Bio-Rad). After giving pulse 1 ml SOC medium was added immediately and sample was incubated at 37^{o}C shaker for 45 min. Then sample was plated on LB agar containing streptomycin (75µg/ml) and kanamycin (50 µg/ml). Plates were incubated overnight at 37^{o}C.

3.1.1. Error Prone Polymerase Chain Reaction (PCR)

LS, containing heterotetramer formation defective R88A mutation was subjected to error prone PCR in mutagenic PCR mix with suitable forward and reverse primers (Appendix E). Mutagenic PCR mix includes 1X Taq polymerase buffer, 1mM ATP and

GTP, 0.02 mM CTP and TTP, 3 mM $MgCl_2$ and 0.4 mM $MgSO_4$. Reaction was performed with 50 ng plasmid pML7 (Appendix D) containing LS_{R88A} under these conditions: at 94^{o}C 30 sec, 50 ^{o}C 30 sec and 72^{o}C 2 min, 15 cycles. The aim was to mutate at least 1 or 2 extra residues.

3.1.2. Cloning

pML7 plasmid containing LS_{R88A} gene was used as vector in the cloning process which is obtained via midiprep kit (Axygen)

Subsequently, error prone PCR products were cleaned up by phenol chloroform isoamyl alcohol extraction. Mutant library and pML7 plasmid were cut by NcoI and HindIII restriction enzymes at 37^{o}Cand for 4 hours and afterwards ligated at 16^{o}C for 12 hours. A control ligation reaction lacking insert DNA was also preformed in order to estimate the amount of background ligation products. Products of ligation were transformed into chemically competent DH5α *E.coli* cells and plated on LB agar plates containing 50µg/ml spectinomycin. After overnight incubation at 37^{o}C cells containing mutant library were scraped and pooled in an LB medium. Those cells were subjected to plasmid isolation (AxyPrep™ Plasmid Miniprep Kit) in order to obtain mutant library.

3.2. Screening and Selection

To screen and select suppressor mutants, isolated mutant LS library containing pML7 plasmids were sequentially transformed into *E. coli* AC70R1–504 ($glgC^{-}$), carrying the SS cDNA expression plasmid pML10 (Appendix D). The particular contribution of each mutant to LS-SS interaction was evaluated by their ability to complement the $glgC^{-}$ mutation and synthesize glycogen on Kornberg medium enriched

with 2% glucose containing 75 μg/ml streptomycin and 50 μg/ml kanamycin. Glycogen accumulation of phenotypes was detected by iodine staining via subjecting plates to iodine beads (Sigma) for 1 min. Approximately, in 8000 colonies 20 colonies were able to synthesize glycogen as I_2 staining revealed. Each stained colony was picked and subjected to plasmid isolation.

3.3. Identification of Second Site Revertant Mutations by Sequence Analysis

Isolated plasmids containing suppressor mutations were amplified by PCR and sent to sequencing. Locations of mutations were determined by BLAST analysis.

3.4. Site Directed Mutagenesis

R88A mutations of selected second site revertants were reversed to its wild type form Ala to Arg in order to see the effects of those mutations in the absence of R88A mutation. Target cDNAs were subjected to site directed mutagenesis PCR with the appropriate primer set (Appendix E). The PCR condition was as follows, 50 ng template cDNA, 30 pmol pirmer set, 0.2 mM dNTPs, 1.5 mM $MgCl_2$ and 1x Dream Taq buffer at 94^{o}C 30 sec, 50^{o}C 30 sec, 68^{o}C 12 min and for 14 cycles. After PCR, DpnI digestion was done to get rid of former template. Then, PCR products were transformed into chemically competent DH5α *E.coli* cells, plated onto LB agar spectinomycin (50μg/ml) plates and incubated overnight at 37^{o}C. The presences of the mutations were confirmed with BLAST analysis after sequencing.

3.5. Specific Activity Measurements

3.5.1. Protein Expression

AC70R1–504 (glgC$^-$) cells were grown in 25 ml of LB medium and then induced with 10 mg/L of nalidixic acid and 200 mM isopropyl- b-D-thiogalactopyranoside (IPTG) at room temperature for 20 h when the culture OD600 reached 1–1.2. The cells were harvested by centrifugation and disrupted by sonication in 1 ml lysis buffer [16Trwas-buffered saline (TBS), 200 mg/ml lysozyme, 5 mg/ml protease inhibitor (Sigma), and 1 mM phenylmethylsulfonyl fluoride (PMSF) (Roche)]. The crude homogenate was centrifuged at 14,000 g for 10 min. The resulting supernatant was used. Protein levels were determined by Bradford assay according to the manufacturer's (Bio-Rad) instructions (Bio-Rad Laboratories, CA, USA).

3.5.2. Specific Activity Assay of Crude Extracts (reverse direction)

A nonradioactive endpoint assay was used to determine the amount of Glc-1-P produced by coupling its formation to NADPH production using phosphoglucomutase and Glc-6-P dehydrogenase (Sowokinos, 1976). Standard reaction mixture contains 100 mM HEPES (pH 7.4), 4 mM DTT, 5 mM 3PGA, 5 mM $MgCl_2$ 3 mM $NaPP_i$, 1 mM ADP-Glucose in a 250 ul reaction volume. Reactions were initiated by enzyme addition, incubated at 37^{o}C for 10 min and stopped by boiling for 2 min. After termination, 350 ul dH_2O was added and mixture was clarified by 5 min centrifugation. 500 ul of clarified supernatant was transferred in a new tube and 500 ul development mixture containing 3 mM NADP, 1 U phosphoglucomutase and 1 U Glc-6-P dehydrogenase was added. Absorbance was recorded at 340 nm. The amount of Glc-1-P produced was determined from a standard curve using freshly prepared Glc-1-P in

complete reaction mixtures and omitting enzyme. Specific activity was defined as a unit/mg protein, whereby 1 unit was defined as 1 umol/min.

3.6. Partial Purification

Proteins were expressed in 1 L LB medium, as described in 3.5.1. Harvested cells first washed once with TBS. The resulting cell pellet was resuspended in buffer A (50 mM Tris-HCl pH 8.0, 10% glycerol, 5 mM $MgCl_2$) containing 200 μg/ml of lysozyme, 5 mg/ml protease inhibitor cocktail and 1 mM PMSF. Resuspended cells were incubated on ice for 20 min and then were disrupted by sonication. Cell debris was removed by centrifugation at 14000 rpm for 30 min, the supernatant was collected and then enzyme subjected to purification steps.

The clarified cell extracts were subjected to heat shock at 55^{o}C for 5 min with gentle mixing and centrifuged at 14000 rpm for 40 min. The supernatant was then subjected to 30-55% ammonium sulfate fractionation where the resulting precipitate was resuspended in 1 ml of buffer A and desalted by dialysis. The desalted sample was applied to Macro-Prep DEAE weak anion exchange support previously equilibrated with buffer A. The enzyme was eluted from the column by 60 ml linear gradient of buffer A (0 to 0.5 M NaCl). Fractions contained enzyme activity were pooled and stored at -80^{o}C after freezing in liquid nitrogen.

3.7. Kinetic Characterization

Kinetic characterization was done in the forward direction as described in Hannah 2005. The amount of PP_i production was determined with a nonradioactive endpoint assay by monitoring NADH concentration decrease using PP_i reagent (P-7275 Sigma). Reaction mixture contained 50 mM HEPES, pH 7.4, 15 mM $MgCl_2$, 4.0 mM

ATP and 4 mM G1P in a total volume of 200 ul. Assays were initiated by enzyme addition, reactions were performed at 37^{o}C for 10 min and terminated by boiling for 2 min. After adding 300 ul PPi reagent (1 bottle dissolved in 22.5 ml), NADH decrease was monitored at 340 nm. Blank samples were complete reaction mixtures without enzyme. PP_i production was determined from a standard curve using increasing amounts of PP_i in complete reaction mixtures without enzyme.

K_m values were determined in reaction mixtures in which one substrate or effector was added in varying amounts and other reaction components saturated. Saturating amount of G1P, ATP and 3PGA was 4mM, 4mM and 5 mM respectively. 0.04 µg partially purified enzyme was used in the each reaction. V_{max} and K_m values were obtained by nonlinear regression analysis using the Prism software program (Graph Pad, San Diego, CA). The K_i for P_i was determined in the presence of 0.1 mM 3PGA, 0.25 mM 3PGA adding increasing amounts of P_i.

3.8. SDS-PAGE and Western Blotting

Electrophoretic separation and analysis of the proteins for confirmation of expression and purification steps were performed by SDS-PAGE following by western blotting. Protein samples were electrophoresed on a 10% SDS-PAGE. Gels subjected to 150 V for 1.5 h for the separation of proteins. Then, gel was transferred to polyvinylidene difluoride membrane (Biotrace PVDF, Pall Corporation, FL, and USA) with transfer cell at 90V for 1h. After pre-blocking with BSA, the membrane was incubated with anti-LS or anti-SS (1:1000 diluted in 0.01 % Tween20/ TBS) and anti rabbit-HRP conjugated secondary antibody (1:5000 diluted in 0.01% Tween20/ TBS) for 1 h, respectively. Proteins were visualized by ECL system.

Chapter 4

RESULTS

4.1. Error Prone PCR

Error prone PCR was performed using LS_{R88A} as template DNA in the presence of unequal molar of dNTPs and Mn^{+2}. PCR products' formation was controlled using 1% agarose gel. As can be seen in Figure 4.1, the PCR products were obtained around 1.5 kb, which indicates error prone PCR successfully worked under defined conditions without having any nonspecific products. In order to find second-site revertants, the next step was cloning of the PCR products into bacterial expression vector, pML7.

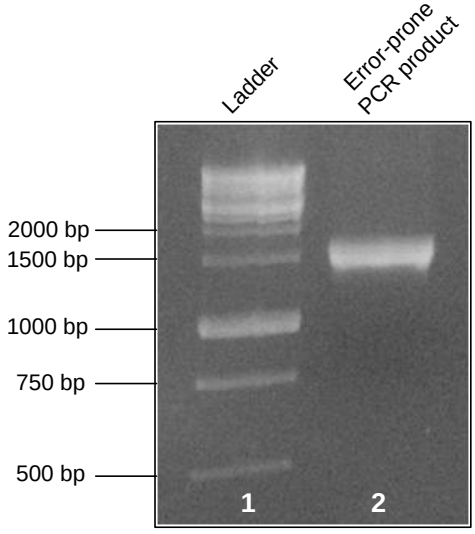

Figure 4.1 Error prone PCR product on 1 % agarose gel. The length of the product is 1500 bp. Lane 1 and lane 2 show ladder and the error prone PCR product, respectively.

4.2. Preparation of the Mutant Library

To confirm pML7, that already bears LS_{R88A} coding sequence of AGPase was subjected to restriction digestion using NcoI and HindIII enzymes and restriction digestion products were run on agarose gel (%1). The presence of two bands around 1.5 kb and 4.5 kb (Figure 4.2 lane 2) indicated that pML7 contains LS_{R88A} and completely digested. By this way, LS_{R88A} coding sequence was removed from the plasmid and digested pML7 was isolated from the gel. PCR products resulted from error prone PCR were also subjected to restriction digestion with the same enzymes and isolated from agarose gel. Finally, digested and gel purified error prone PCR product were ligated into digested and gel purified pML7 vector at the appropriate restriction sites. Then ligation products were transformed into DH5α *E. coli* cells which resulted in total 7500 transformants except background transformants. Then all these transformants were collected and subjected to the plasmid purification to obtain mutant LS library. Next, isolated library plasmids were transformed to the *E.coli* cell ($glgC^-$) harboring wild type cDNA of small subunit of AGPase in pML10 vector to find second site revertants from this library. So, the next step was the identification of the revertants by iodine staining.

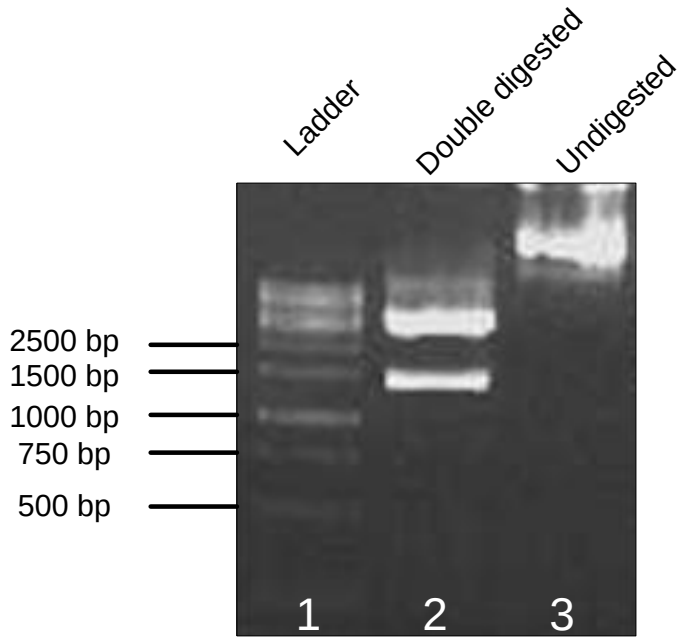

Figure 4.2 Control of the digestion of the pML7 vector containing LS. Lane next to ladder contains double digested midiprep product and last lane is the undigested form of purified pML7.

.

4.3. Screening and Selection of the Second Site-Revertant

Selection of the second-site revertants was accomplished by complementation of the potato SS and LS cDNAs to the bacterial glgC$^-$ gene in the AGPase deficient *E.coli* AC70R1-504 strain. The ability of the LS mutants to form a functional heterotetrameric AGPase was assessed by exposing mutant colonies to I_2 vapor to monitor the glycogen accumulation. Since the mutant used in this study cannot form a stable heterotetramer AGPase as reported previously, we assumed that any cells that contain second-site mutation(s) in LS will restore glycogen production when they stain with I_2 vapor. Screening of approximately 20000 mutants by I_2 staining revealed that 20 colonies restored glycogen production. In order to identify the nature of second site mutations plasmids of LS were isolated and subjected to sequencing. Sequence analysis (Appendix A) showed that we obtained 15 different revertants from the mutant LS

library. Positions, wild type residues and revertant residues of each mutant are listed in Table 4.1.

Since investigation of the role of the subunit interaction for the heterotetramer formation and allosteric regulation of the AGPase is the starting point of this study, we further analyzed the sequences according to their relative location to the subunit interface residues. Figure 4.3 depicts both subunit interface residues (gray highlighted) and revertant residues obtained in this study (marked with colored arrows). As seen in Figure 4.3, seven residues among randomly mutated residues are exactly located at the subunit interface. In addition, five residues have close proximity to the subunit interface residues. Mutations of RM2, RM7, RM25, RM27 and RM29 are located on the subunit interface. RM11 and RM16 have mutations which are not exactly located on the subunit interface but they are close to them considerably. In addition, although some residues (such as D410 residue of RM10) seem far away from the subunit interface residues, their locations seem close to subunit interface when they put onto the heterotetrameric model of the potato AGPase (Appendix B).

Table 4.1 Positions of the randomly mutated revertant residues as sequence analysis revealed

Clone	Wildtype Residues	Position	Revertant residues	Clone	Wildtype Residues	Position	Revertant residues
RM2	Ile Glu Tyr	90 287 378	Val Lys Cys	**RM16**	Asp Phe Glu	184 311 358	Glu Leu Gly
RM4	Ile Asn	62 418	Val Ser	**RM20**	Val Ile	223 236	Ala Asn
RM5	Asp Thr	219 291	Val Ala	**RM22**	Arg Val	200 419	Glu Ala
RM6	Pro	395	Leu	**RM25**	Arg Val Ile	200 419 90	Glu Ala Val
RM7	Tyr Asp	378 410	His Gly	**RM27**	Ala Phe Ile Asn Asn Asp	91 101 330 332 401 410	The Leu The Lys Asp Gly
RM10	Asp	410	Gly	**RM28**	Phe Met	345 373	Ser Val
RM11	Glu	138	Gly	**RM29**	Phe	95	Leu
RM13	Val	202	Ala				

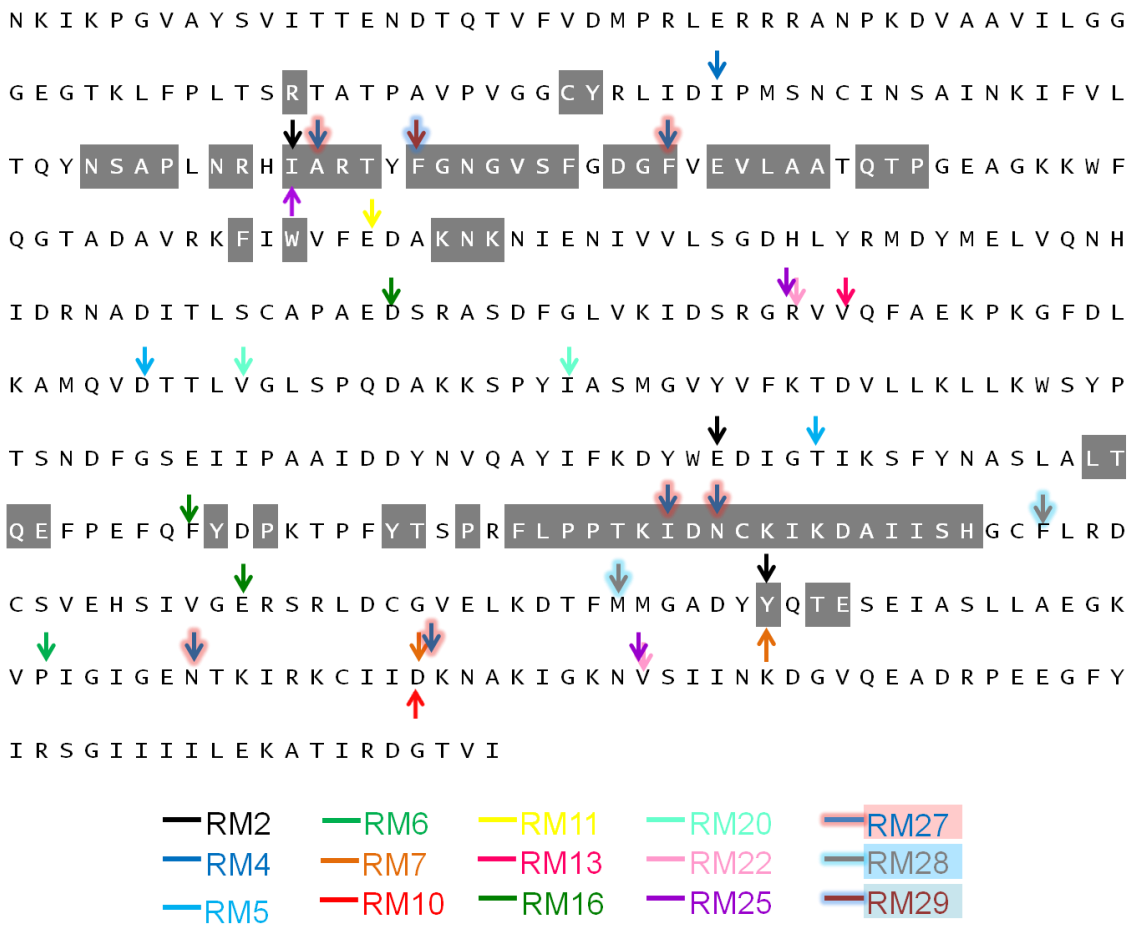

Figure 4.3 Amino acid sequence of wildtype potato LS (accession no. Q00081.1). gray highlighted region indicate sites that make direct contact with the SS as determined by Tuncel et al. (2008). Location of the random mutations were indicated in the figure with colored arrows.

4.4. Site Directed Mutagenesis

To assess the effects of the second-site mutants independently original mutant Ala88 was replaced with wild type Arg by site directed mutagenesis to see whether the obtained revertant residues enhance heterotetramer formation of the enzyme or affect kinetic and regulatory properties of AGPase. For this reason, Figure 4.4 shows a representative result of the performed site directed mutagenesis in which 6 kb PCR product is seen on the lane 2. Each random mutant was subjected to the site directed mutagenesis and the result was confirmed with sequencing.

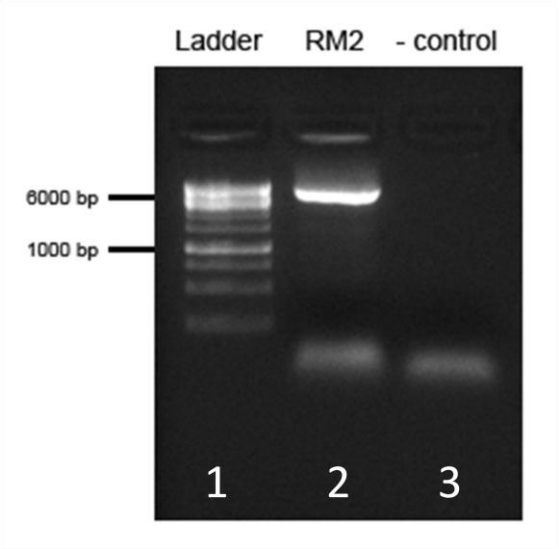

Figure 4.4 Site directed mutagenesis PCR check on the agarose gel. Negative control was the PCR product lacking DreamTaq polymerase (lane 3).

4.5. Characterization of Mutants by Iodine Staining

Second site suppressor mutants were initially compared based on their glycogen synthesis by production of brown staining colonies following exposure to iodine vapor. Since more stained bacteria with iodine means more glycogen production, iodine staining was used as initial determinant to select colonies that will be further characterized. Therefore, cells were grown on Kornberg medium containing 2% (w/v) glucose and grown colonies were exposed to iodine beads for 1 min. Figure 4.5 shows the iodine staining comparison of the revertant mutants in which RM2 showed the most significant staining among random mutants. Some of the mutants (RM5 and RM 29) didn’t display high glycogen accumulation in heterologous system, while some mutants (RM10, RM7, RM11 and RM6) stained with a comparable amount relative to the wild type cells.

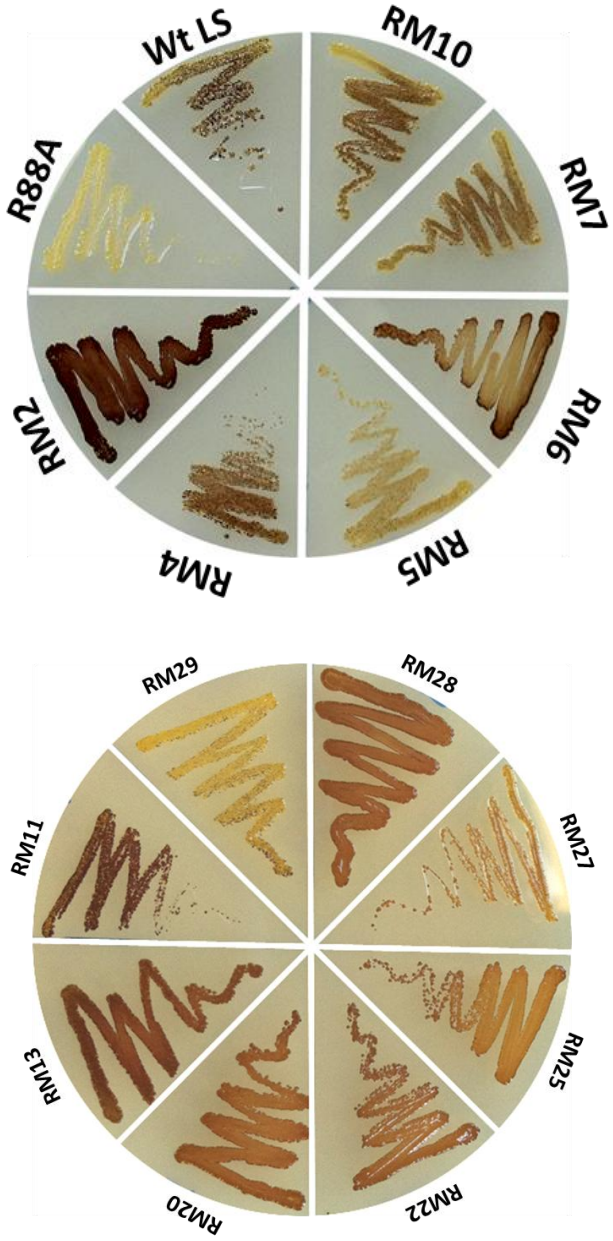

Figure 4.5 Iodine staining of the revertant residues. Qualitative determination of the AGPases activity according to the glycogen production levels

4.6. Specific Activity Measurements

Specific activities of mutants were measured to see whether they displayed enhanced enzyme activity in the crude extracts. Therefore, cells that contain the mutant LS plasmid and the wild type SS were successfully expressed in 25 mL of liquid LB. To see expression of the mutant LSs western blot analysis was performed on the crude extracts of samples (Figure 4.6). Then, specific activities of the soluble fractions of crude extracts were monitored in the reverse direction of the AGPase reaction using saturating amounts of substrates and activator. Figure 4.7 depicts the specific activities of wild type LS, LS_{R88A} and some selected revertant residues. Among those revertant residues RM7 and RM10 have comparatively higher specific activity than the wild type LS. In addition, RM2 has the closest value of the specific activity to the wild type LS. Interestingly, although RM6, RM11 stained comparable amounts to the wild type they showed relatively low specific activity. On the other hand RM22 and RM25 confirm the low glycogen accumulation assessed by I_2 staining with their low specific activity results.

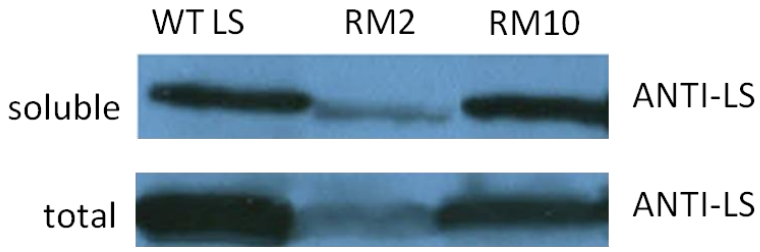

Figure 4.6 Western blot confirmation of the expressed wild type and mutant AGPases. First lane shows soluble fraction and second lane shows total crude extracts of the expressed proteins. AGPase was detected with LS polyclonal antibody.

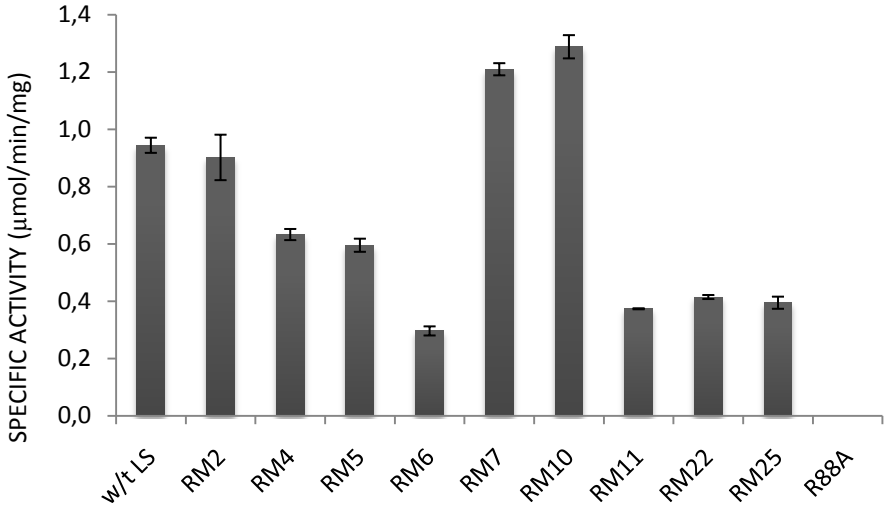

Figure 4.7 Specific activities of soluble fractions of the crude extracts. G1P production was measured with a coupled assay by monitoring NADH production.

4.7. Partial Purification

Based on iodine staining and specific activity results RM2 and RM10 mutants were selected for further biochemical characterization. For this reason, prior to kinetic analysis the wild type AGPase, RM2 and RM10 were partially purified. pML7 and pML10 plasmids carrying mutant/wildtype LS and wildtype SS respectively were successfully expressed in glgC$^-$ cells. After cell harvesting and lysis steps, heat shock, ammonium sulfate precipitation and anion exchange chromatography steps were applied sequentially. Fractions containing the highest specific activity during linear gradient were stored at -80^{o}C. Figures 4.8, 4.9 and 4.10 show the SDS-PAGE analysis of the partially purified wild type LS/SS, RM2/SS and RM10/SS AGPases respectively. Bands around 50 kDa are the desired partially purified products which are indicated

with black arrows on the figures. As seen on the figures partial purification provided to get rid of most of the unwanted proteins. Table 4.2 summarizes results obtained in the partial purification. Wild type and mutant forms were obtained 6 to 8 fold purified form with approximately 10% yield ratio.

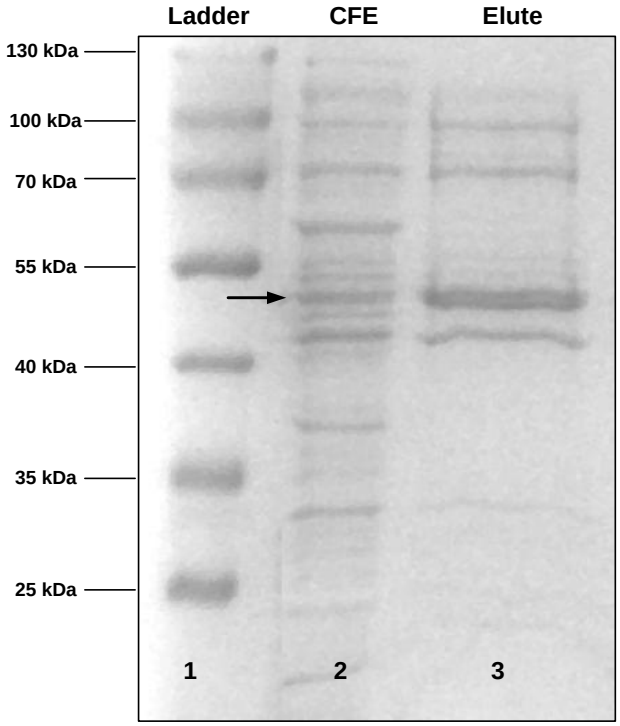

Figure 4.8 SDS-PAGE analysis of partial purification of the wild type LS/SS. The progress of purification was monitored with SDS-PAGE by Coomassie blue staining by loading cell free extracts and fractions having highest specific activity. Black arrow depicts the position of the partially purified protein which is around 50 kDa.

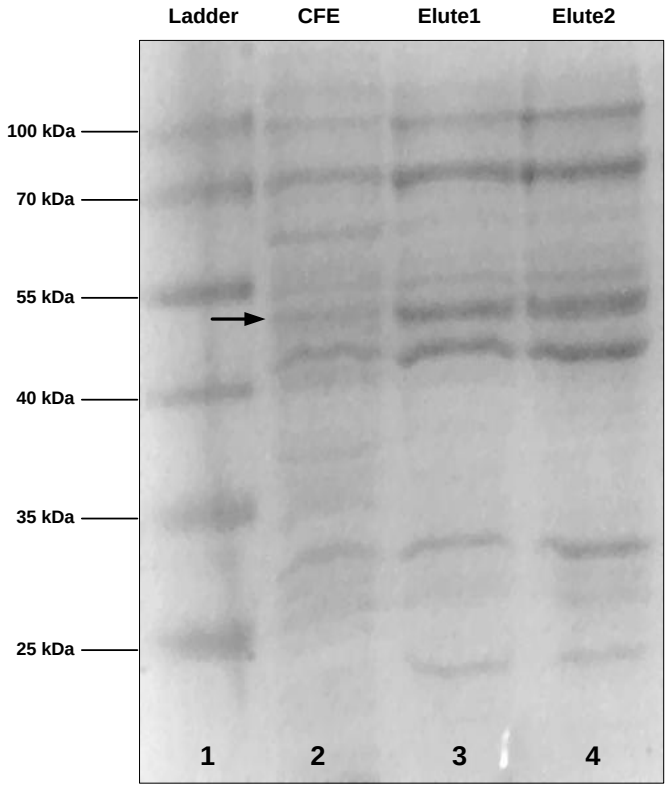

Figure 4.9 SDS-PAGE analysis of purification of the revertant mutant RM2/SS. The progress of purification was monitored with SDS-PAGE by coomassie blue staining by loading cell free extracts and fractions having highest specific activity. Black arrow depicts the position of the partially purified protein which is around 50 kDa.

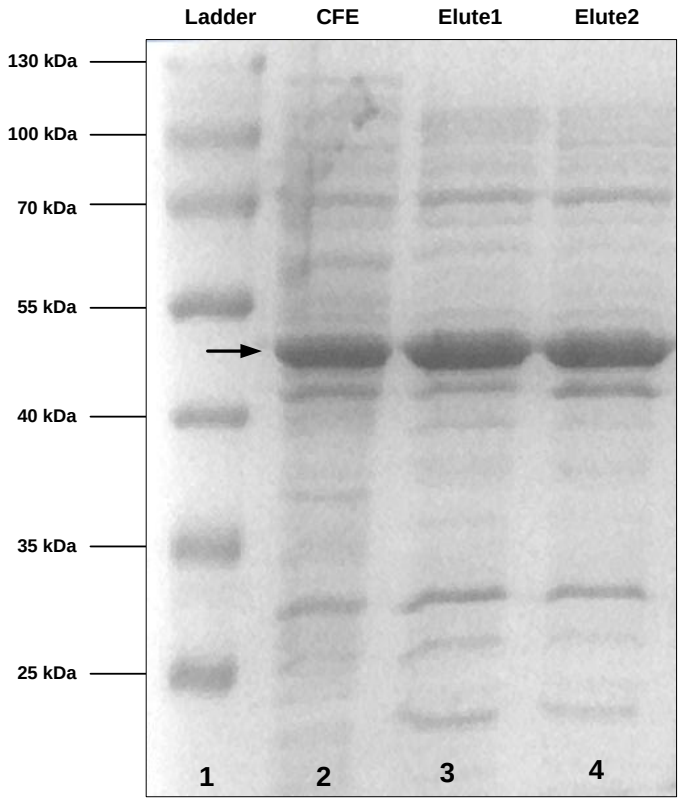

Figure 4.10 SDS-PAGE analysis of purification of the revertant mutant RM10/SS. The progress of purification was monitored with SDS-PAGE by coomassie blue staining by loading cell free extracts and fractions having highest specific activity. Black arrow depicts the position of the partially purified protein which is around 50 kDa.

Table 4.2 Partial purification of the wild type LS, RM2 and RM10

Assays were performed in the reverse direction by monitoring G1P production. 1 unit is defined as 1µmol/min. This table includes only CFE and elutes from DEAE anion exchange chromatography. Heat shock and ammonium sulfate steps were not determined since they were monitored in the prior optimization steps.

	Volume (ml)	*Protein (mg)*	*Activity (units)*	*Specific Activity (unit/mg)*	*Fold Purification*	*Yield (%)*
Wt LS – CFE	30	48	35.6	0.74	1	100
Wt LS – Elute	1.5	0.65	4	6.03	8.1	10.9
RM2 – CFE	15	120	27.3	0.23	1	100
RM2 – Elute1	1.5	2.5	3.98	1.56	6.9	14.6
RM2 – Elute2	1.5	3	3.2	1.3	5.6	11.7
RM10 – CFE	14	120	71.5	0.59	1	100
RM10 – Elute1	1.5	2.4	7.76	3.23	5.4	10.8
RM10 – Elute2	1.5	3	7.72	2.25	4.3	10.8

4.8. Kinetic Characterization

RM2 and RM10 revertant mutants were selected for further kinetic characterization according to their iodine staining and specific activity results. RM2 is the most significant stained mutant and it showed a specific activity level similar to the wild type enzyme. RM10 also stained considerably and it showed higher specific activity than wild type. Kinetic characterization provided us to determine the effect of the mutations that we obtained whether they enhance the heterotetramers of the AGPase by increasing subunit interaction or they influence the kinetic and regulatory properties of the enzyme. Their kinetic parameters were analyzed using a spectrophotometric assay which measures the PP_i production with coupled system monitoring NADH decrease.

Kinetic and regulatory properties of RM2, RM10 and wild type AGPases were shown in Table 4.3 (for the individual graphs see Appendix C). K_m values for G1P, ATP and Mg^{2+} were determined for all variants in the presence of 5 mM 3PGA. Both RM2 and RM10 have similar affinities to the substrates ATP and G1P and to the cofactor Mg^{2+}. By contrast, allosteric regulatory properties varied considerably among RM2 and RM10. While RM2 has two fold higher K_a than the wild type, RM10 has almost 4 fold increase in K_a for 3PGA (Figure 4.11). In addition, RM2 has 2 fold increase in resistance to P_i. On the other hand, RM10 is almost five fold intolerable to the P_i inhibition than the wild type AGPase (Figure 4.12).

Table 4.3 Kinetic parameters of the wild type, RM2 and RM10

Kinetic and regulatory properties were determined in the ADP glucose synthesis direction. All values are in mM. K_m and K_a for substrates/cofactor and 3PGA, respectively, correspond to the concentration of these molecules required for the enzyme activity to attain 50% of maximal activity. K_i is the amount of P_i required to inhibit the enzyme activity by 50% of maximal activity.

	Wild type	***RM2***	***RM10***
ATP (K_m)	0.068	0.089	0.085
G1P (K_m)	0.041	0.034	0.043
Mg^{2+} (K_m)	3.6	3.4	3.7
3PGA (K_a)	0.12	0.28	0.41
P_i (K_i, 0.25 mM 3PGA)	0.19	0.36	0.04

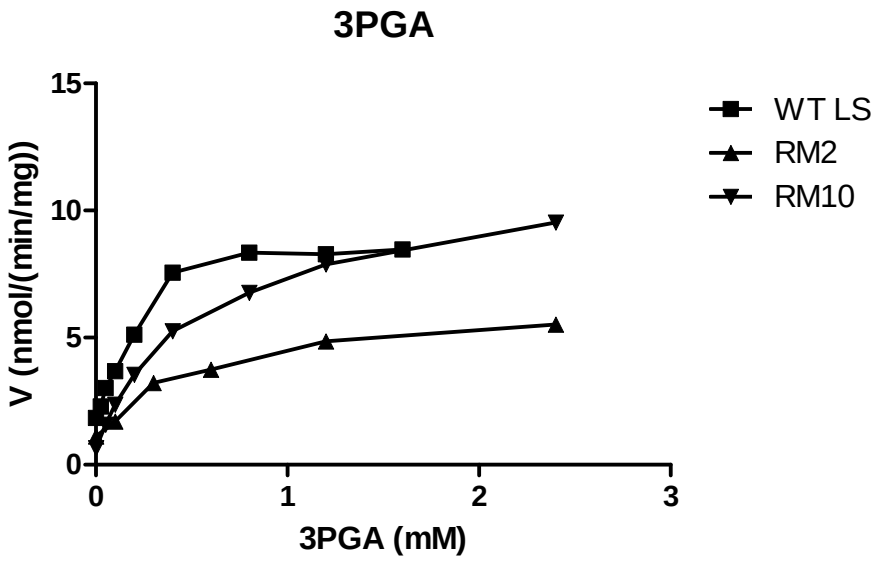

Figure 4.11 3PGA activation graph of the wild type AGPase and mutants RM2 and RM10.

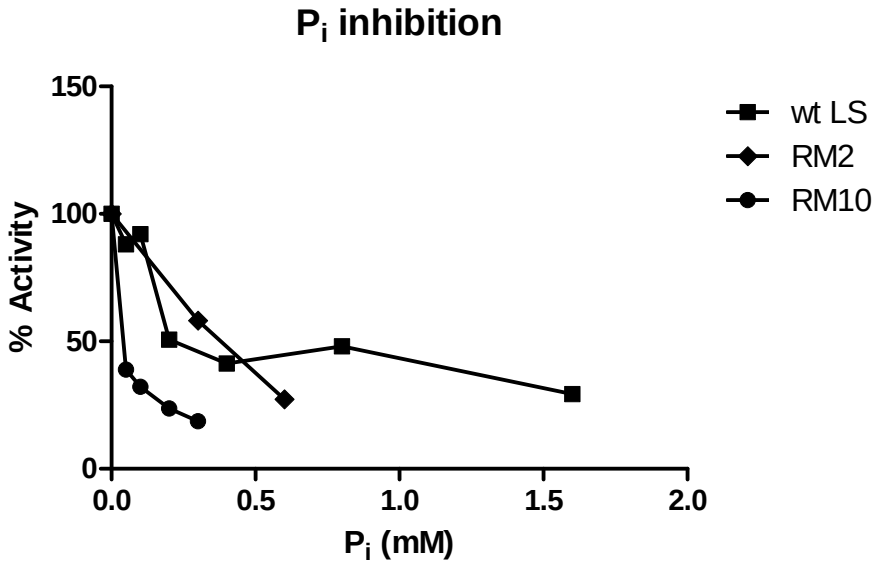

Figure 4.12% activity inhibition of P_i of the wild type AGPase and mutants RM2 and RM10

Chapter 5

DISCUSSION

AGPase has been extensively studied in order to increase its activity since it is a key enzyme in the starch biosynthesis. Currently, limited structural data is available for the AGPase. Only the crystal structures of the small subunit homotetramer of potato AGPase [40] and homotetrameric AGPase of *A.tumefaciens* [41] has been solved in their inhibited forms. Therefore, deciphering the specific role of the amino acid residues or protein motifs of the AGPase enables to engineering of the AGPase to increase starch yield in crop plants.

Herein, we have identified amino acid residues of LS that are important for the allosteric regulation of the potato AGPase. Reverse genetics and random mutagenesis approaches were applied to identify critical amino acid residues of LS for the investigation of the heterotetrameric interaction and the allosteric regulation of the AGPase. This study focused on the effects of the subunit interaction considering two possible outcomes of the modification of the parts of the enzyme involved in subunit on interaction. Enhancing heterotetrameric AGPase formation by increasing the subunit interaction between LS and SS was the first possible outcome. Since the interaction between the monomeric subunits is weak [34], enhancing this interaction through subunit interface residues may result in more heterotetramers of the enzyme. Heterotetrameric model of the potato AGPase revealed that longitudinal interaction is weaker than lateral interaction [45]. This implies one should focus on to strengthen the longitudinal interaction. Hence, we chose R88A mutant for this study which disrupts heterotetramer formation probably by inhibiting longitudinal interaction. The second potential outcome was to see different kinetic and allosteric properties in the random mutants due to the changes in critical amino acid residues for the enzyme activity and regulation. The role of the AGPase subunit interfaces in the allosteric regulation of the

enzyme was revealed by Georgelis et al. [46]. In that study, amino acid residues chosen via phylogenetic analysis were mutated and several residues showed altered allosteric properties which are located at the direct contact interface of LS and SS according to the modeled maize endosperm AGPase.

In our study, we subjected the heterotetramer formation deficient LS_{R88A} to random mutagenesis for the reasons discussed above. Obtained randomly mutant LS library was screened for the ability to form an enzyme displaying glycogen production in glgC$^-$ *E.coli* cells. Screening via iodine staining identified 15 different revertant mutant forms of the LS. Among those revertants according to the iodine staining and specific activity measurements of the crude extracts, we selected two mutants named RM2 and RM10 for further biochemical characterization. For this reason RM2, RM10 and the wild type AGPases were partially purified and their kinetic and allosteric properties were analyzed and compared.

Although substrate and cofactor affinities did not show any significant change relative to the wild type enzyme, allosteric properties of the mutants RM2 and RM10 showed notable differences. While RM2 has two fold higher K_a than the wild type, RM10 has almost 4 fold increase in K_a for 3PGA. Moreover, RM10 is inhibited with much less amounts of P_i than the wild type enzyme. However, RM2 is inhibited in the presence of 2 fold more P_i relative to the wild type AGPase which means RM2 is more tolerable to P_i inhibition than the wild type. Interestingly, two mutations of the RM2, I90V and Y378C, are located at the subunit interface of the tetrameric enzyme (Fig 4.4 and model of RM2 in Appendix B). For the case of RM10, although the D410G mutation is not located at the subunit interfaces of the modeled structure, it seems very close to the R88 residue on simulation of the model (Appendix B, RM10). Since Aspartic acid changed to more flexible Glycine residue, this side chain change probably affects the subunit interaction and so the allosteric properties. Further computational analysis may be required to provide evidence and insight for this change. In addition, 410th Aspartic acid residue seems to have a significant role for the allosteric regulation as the P_i inhibition and 3PGA activation results indicated. Since SDS-PAGE and Native

PAGE analysis of the RM2 and RM10 did not show a significant increase in the heterotetramer amount of the enzyme (data not shown), we can conclude that mutations that we obtained support our second outcome which is indicated above. In other words, these results demonstrate that the subunit interaction between the SS and LS is not only required for heterotetrameric enzyme formation but also significant for the allosteric regulation of the enzyme. Previously the role of functional interaction between LS and SS for the allosteric properties was shown [21, 60]. Nonetheless, until now only one study showed that the subunit interface residues are important for the allosteric regulation by a phylogenetic analysis [46]. So, our study not only supported that study but also introduced new residues located at the subunit interface that are significant for the allosteric regulation of the AGPase.

As seen in Figure 4.4 seven mutations exactly place on the subunit interfaces of the modeled heterotetrameric AGPase. Four of them belong to the RM27 mutant form of the LS. Since RM27 contains six random mutations and it did not reveal a significant I_2 staining, its kinetic characterization was not performed. Surprisingly, two of the random mutations of RM27, A91T and F101L, were previously identified as significant residues for the allosteric regulation of the maize endosperm AGPase by Georgelis et al. [46]. In that study, mutating Ser residue of the maize endosperm AGPase to the corresponding Phe residue of the potato LS resulted in significant changes in the kinetic and allosteric properties of the maize AGPase. Additionally two other mutations of the RM27, I330T and N332K, are located on the subunit interfaces of the heterotetrameric model of the AGPase (Appendix B, RM27). Ile330 was previously identified as a hot spot for the lateral interaction by our group [4]. Those results show that in fact, RM27 contains critical mutations which are located at subunit interfaces. However, RM27 has too many mutations that one mutation could negatively affect to the other mutation. Therefore mutations of the RM27 should be further analyzed individually or combinatorially. This approach is also valid for the other randomly mutant forms of the LS obtained in this study. Mutations located at the interface or nearby of the interface residues may be analyzed computationally and if a significant effect is seen that

combination of different mutations should be introduced to LS and then characterized. One of those combinations may result with an enhanced heterotetrameric AGPase or up-regulated form of the AGPase, since the subunit interaction takes a significant role for these processes. Additionally, the allosteric sites detected in this study can also be targets of different mutagenesis studies to obtain variants which are activated by low 3PGA and inhibited by high P_i concentrations. These kinds of further studies may provide to obtain potato AGPase variants which will have agronomic benefits.

All in all, this study enhanced our understanding of how the subunit interaction effects to the allosteric regulation of the potato AGPase and led up to further future studies for the engineering of the AGPase with the aim of increased starch yield in the crop plants.

Chapter 6

CONCLUSION

Starch is not only a fundamental storage polysaccharide of plants but also the major carbohydrate in the human diet and significant raw material for the industry. Therefore increasing starch yield is one of the highlighted issues of science. One of the approaches to increase starch yield focuses on engineering of ADP Glucose Pyrophosphorylase (AGPase). AGPase catalyzes the first committed step of the glycogen synthesis in bacteria and the starch synthesis in algae and plants.

Plant AGPase is a heterotetrameric enzyme consisting of two large and two small subunits. Large subunit modulates catalytic activity of the small subunit by allosteric regulation. 3PGA/P_i ratio is responsible from the allosteric regulation of the enzyme in which increase of 3PGA concentration activates enzyme and increase of P_i concentration inhibits the enzyme activity.

In this work, we concentrated on subunit interaction between LS and SS of the potato AGPase for two reasons. Enhancing heterotetrameric assembly through modifying subunit interface residues is the first one. The second one is to find out the role of subunit interaction on the allosteric regulation of the AGPase. Hence, reverse genetics and random mutagenesis approaches were applied to the heterotetramer formation deficient mutant LS_{R88A}. In this context, a randomly mutant LS library was obtained via error prone PCR, cloned and screened for the phenotypes that are capable of restoring glycogen production in $glgC^-$ *E.coli* cells by iodine staining. 15 revertant mutant forms of LS were obtained. Then, R88A mutation was reversed to its wild type form to eliminate its adverse effects on the tetramer formation. Obtained mutants were first analyzed based on their iodine staining and specific activity levels and RM2 and RM10 were selected for further characterization. Although a significant increase in the

heterotetramer amount did not obtained, RM2 and RM10 revealed altered allosteric properties than the wild type AGPase.

Altered allosteric properties of the mutants are important since they directly designate the significance of the subunit interface residues for the allosteric regulation of the enzyme. Since exact 3D structure of the functional AGPase is still not known these kinds of identifications set the stage for engineering of the AGPase for more starch yield.

Future work for this study should be the further characterization of the other mutants. As many random mutations were identified at or near subunit interfaces, their combinatorial introduction to the LS may result in enhanced AGPase by means of increase in heterotetramer formation or up regulation of the enzyme. Besides, type of the existing mutations may be changed to other type of amino acid residues if there is a better option. This change may also provide improvements including heat stability, specific activity for the enzyme. Combination of the results of this study with a computational study may serve as guidance to obtain better AGPase variants.

BIBLIOGRAPHY

1. Slattery, C.J., I.H. Kavakli, and T.W. Okita, *Engineering starch for increased quantity and quality.* Trends in Plant Science, 2000. **5**(7): p. 291-298.
2. Zeeman, S.C., J. Kossmann, and A.M. Smith, *Starch: its metabolism, evolution, and biotechnological modification in plants.* Annu Rev Plant Biol, 2010. **61**: p. 209-34.
3. Ballicora, M.A., et al., *Adenosine 5'-Diphosphate-Glucose Pyrophosphorylase from Potato-Tuber - Significance of the N-Terminus of the Small-Subunit for Catalytic Properties and Heat-Stability.* Plant Physiology, 1995. **109**(1): p. 245-251.
4. Baris, I., et al., *Investigation of the interaction between the large and small subunits of potato ADP-glucose pyrophosphorylase.* PLoS Comput Biol, 2009. **5**(10): p. e1000546.
5. Zeeman, S.C., S.M. Smith, and A.M. Smith, *The diurnal metabolism of leaf starch.* Biochem J, 2007. **401**(1): p. 13-28.
6. Salehuzzaman, S.N., E. Jacobsen, and R.G. Visser, *Isolation and characterization of a cDNA encoding granule-bound starch synthase in cassava (Manihot esculenta Crantz) and its antisense expression in potato.* Plant Mol Biol, 1993. **23**(5): p. 947-62.
7. Buleon, A., et al., *Starch granules: structure and biosynthesis.* Int J Biol Macromol, 1998. **23**(2): p. 85-112.
8. Hizukuri, S., *Polymodal distribution of the chain lengths of amylopectins, and its significance.* Carbohydrate Research, 1986. **147**(2): p. 342-347.
9. Smith, A.M., *Prospects for increasing starch and sucrose yields for bioethanol production.* Plant J, 2008. **54**(4): p. 546-58.

10. Regierer, B., et al., *Starch content and yield increase as a result of altering adenylate pools in transgenic plants.* Nat Biotechnol, 2002. **20**(12): p. 1256-60.
11. Stark, D.M., et al., *Regulation of the Amount of Starch in Plant Tissues by ADP Glucose Pyrophosphorylase.* Science, 1992. **258**(5080): p. 287-92.
12. Ball, S.G. and M.K. Morell, *From bacterial glycogen to starch: understanding the biogenesis of the plant starch granule.* Annu Rev Plant Biol, 2003. **54**: p. 207-33.
13. Okita, T.W., et al., *The Subunit Structure of Potato Tuber ADPglucose Pyrophosphorylase.* Plant Physiol, 1990. **93**(2): p. 785-90.
14. Ballicora, M.A., A.A. Iglesias, and J. Preiss, *ADP-glucose pyrophosphorylase, a regulatory enzyme for bacterial glycogen synthesis.* Microbiol Mol Biol Rev, 2003. **67**(2): p. 213-25, table of contents.
15. Choi, S.B., et al., *Transcriptional expression characteristics and subcellular localization of ADP-glucose pyrophosphorylase in the oil plant Perilla frutescens.* Plant Cell Physiol, 2001. **42**(2): p. 146-53.
16. Okita, T.W., et al., *Subcellular localization of the starch degradative and biosynthetic enzymes of spinach leaves.* Plant Physiol, 1979. **64**(2): p. 187-92.
17. Nakata, P.A., et al., *Comparison of the primary sequences of two potato tuber ADP-glucose pyrophosphorylase subunits.* Plant Mol Biol, 1991. **17**(5): p. 1089-93.
18. Smith-White, B.J. and J. Preiss, *Comparison of proteins of ADP-glucose pyrophosphorylase from diverse sources.* J Mol Evol, 1992. **34**(5): p. 449-64.
19. Crevillen, P., et al., *The different large subunit isoforms of Arabidopsis thaliana ADP-glucose pyrophosphorylase confer distinct kinetic and regulatory properties to the heterotetrameric enzyme.* J Biol Chem, 2003. **278**(31): p. 28508-15.
20. Preiss, J. and M.N. Sivak, *Biochemistry, molecular biology and regulation of starch synthesis.* Genet Eng (N Y), 1998. **20**: p. 177-223.

21. Cross, J.M., et al., *Both subunits of ADP-glucose pyrophosphorylase are regulatory.* Plant Physiol, 2004. **135**(1): p. 137-44.
22. Salamone, P.R., et al., *Isolation and characterization of a higher plant ADP-glucose pyrophosphorylase small subunit homotetramer.* FEBS Lett, 2000. **482**(1-2): p. 113-8.
23. Gomez-Casati, D.F., J. Preiss, and A.A. Iglesias, *Studies on the effect of temperature on the activity and stability of cyanobacterial ADP-glucose pyrophosphorylase.* Arch Biochem Biophys, 2000. **384**(2): p. 319-26.
24. Ballicora, M.A., A.A. Iglesias, and J. Preiss, *ADP-Glucose Pyrophosphorylase: A Regulatory Enzyme for Plant Starch Synthesis.* Photosynth Res, 2004. **79**(1): p. 1-24.
25. Okita, T.W., *Is there an alternative pathway for starch synthesis?* Plant Physiol, 1992. **100**(2): p. 560-4.
26. Ball, K. and J. Preiss, *Allosteric sites of the large subunit of the spinach leaf ADPglucose pyrophosphorylase.* J Biol Chem, 1994. **269**(40): p. 24706-11.
27. Preiss, J., et al., *Starch biosynthesis and its regulation.* Biochem Soc Trans, 1991. **19**(3): p. 539-47.
28. Kavakli, I.H., et al., *Analysis of allosteric effector binding sites of potato ADP-glucose pyrophosphorylase through reverse genetics.* J Biol Chem, 2001. **276**(44): p. 40834-40.
29. Greene, T.W., et al., *Generation of up-regulated allosteric variants of potato ADP-glucose pyrophosphorylase by reversion genetics.* Proc Natl Acad Sci U S A, 1998. **95**(17): p. 10322-7.
30. Salamone, P.R., et al., *Directed molecular evolution of ADP-glucose pyrophosphorylase.* Proc Natl Acad Sci U S A, 2002. **99**(2): p. 1070-5.
31. Boehlein, S.K., et al., *Characterization of an autonomously activated plant ADP-glucose pyrophosphorylase.* Plant Physiol, 2009. **149**(1): p. 318-26.
32. Ballicora, M.A., et al., *Activation of the potato tuber ADP-glucose pyrophosphorylase by thioredoxin.* J Biol Chem, 2000. **275**(2): p. 1315-20.

33. Ballicora, M.A., et al., *Heat stability of the potato tuber ADP-glucose pyrophosphorylase: role of Cys residue 12 in the small subunit.* Biochem Biophys Res Commun, 1999. **257**(3): p. 782-6.
34. Tiessen, A., et al., *Starch synthesis in potato tubers is regulated by post-translational redox modification of ADP-glucose pyrophosphorylase: a novel regulatory mechanism linking starch synthesis to the sucrose supply.* Plant Cell, 2002. **14**(9): p. 2191-213.
35. Hendriks, J.H., et al., *ADP-glucose pyrophosphorylase is activated by posttranslational redox-modification in response to light and to sugars in leaves of Arabidopsis and other plant species.* Plant Physiol, 2003. **133**(2): p. 838-49.
36. Ballicora, M.A., et al., *Resurrecting the ancestral enzymatic role of a modulatory subunit.* J Biol Chem, 2005. **280**(11): p. 10189-95.
37. Hwang, S.K., S. Hamada, and T.W. Okita, *Catalytic implications of the higher plant ADP-glucose pyrophosphorylase large subunit.* Phytochemistry, 2007. **68**(4): p. 464-77.
38. Kuhn, M.L., C.A. Falaschetti, and M.A. Ballicora, *Ostreococcus tauri ADP-glucose pyrophosphorylase reveals alternative paths for the evolution of subunit roles.* J Biol Chem, 2009. **284**(49): p. 34092-102.
39. Georgelis, N., E.L. Braun, and L.C. Hannah, *Duplications and functional divergence of ADP-glucose pyrophosphorylase genes in plants.* BMC Evol Biol, 2008. **8**: p. 232.
40. Jin, X., et al., *Crystal structure of potato tuber ADP-glucose pyrophosphorylase.* EMBO J, 2005. **24**(4): p. 694-704.
41. Cupp-Vickery, J.R., et al., *Structural analysis of ADP-glucose pyrophosphorylase from the bacterium Agrobacterium tumefaciens.* Biochemistry, 2008. **47**(15): p. 4439-51.
42. Greene, T.W., et al., *Mutagenesis of the potato ADPglucose pyrophosphorylase and characterization of an allosteric mutant defective in 3-phosphoglycerate activation.* Proc Natl Acad Sci U S A, 1996. **93**(4): p. 1509-13.

43. Laughlin, M.J., S.E. Chantler, and T.W. Okita, *N- and C-terminal peptide sequences are essential for enzyme assembly, allosteric, and/or catalytic properties of ADP-glucose pyrophosphorylase.* Plant J, 1998. **14**(2): p. 159-68.

44. Cross, J.M., et al., *A polymorphic motif in the small subunit of ADP-glucose pyrophosphorylase modulates interactions between the small and large subunits.* Plant J, 2005. **41**(4): p. 501-11.

45. Tuncel, A., I.H. Kavakli, and O. Keskin, *Insights into subunit interactions in the heterotetrameric structure of potato ADP-glucose pyrophosphorylase.* Biophys J, 2008. **95**(8): p. 3628-39.

46. Georgelis, N., J.R. Shaw, and L.C. Hannah, *Phylogenetic analysis of ADP-glucose pyrophosphorylase subunits reveals a role of subunit interfaces in the allosteric properties of the enzyme.* Plant Physiol, 2009. **151**(1): p. 67-77.

47. Dickinson, D.B. and J. Preiss, *Presence of ADP-Glucose Pyrophosphorylase in Shrunken-2 and Brittle-2 Mutants of Maize Endosperm.* Plant Physiol, 1969. **44**(7): p. 1058-62.

48. Tsai, C.Y. and O.E. Nelson, *Starch-deficient maize mutant lacking adenosine dephosphate glucose pyrophosphorylase activity.* Science, 1966. **151**(708): p. 341-3.

49. Muller-Rober, B., U. Sonnewald, and L. Willmitzer, *Inhibition of the ADP-glucose pyrophosphorylase in transgenic potatoes leads to sugar-storing tubers and influences tuber formation and expression of tuber storage protein genes.* EMBO J, 1992. **11**(4): p. 1229-38.

50. Leterrier, M., et al., *Cloning, characterisation and comparative analysis of a starch synthase IV gene in wheat: functional and evolutionary implications.* BMC Plant Biol, 2008. **8**: p. 98.

51. Tomlinson, K. and K. Denyer, *Starch synthesis in cereal grains.* Advances in Botanical Research, Vol 40, 2003. **40**: p. 1-61.

52. Clarke, B.R., et al., *The relationship between the rate of starch synthesis, the adenosine 5'-diphosphoglucose concentration and the amylose content of starch in developing pea embryos.* Planta, 1999. **209**(3): p. 324-9.

53. Lloyd, J.R., et al., *The influence of alterations in ADP-glucose pyrophosphorylase activities on starch structure and composition in potato tubers.* Planta, 1999. **209**(2): p. 230-238.

54. Kossmann, J. and J. Lloyd, *Understanding and influencing starch biochemistry.* Crit Rev Biochem Mol Biol, 2000. **35**(3): p. 141-96.

55. Raemakers, K., et al., *Improved cassava starch by antisense inhibition of granule-bound starch synthase I.* Molecular Breeding, 2005. **16**(2): p. 163-172.

56. Visser, R.G.F., et al., *Inhibition of the Expression of the Gene for Granule-Bound Starch Synthase in Potato by Antisense Constructs.* Molecular & General Genetics, 1991. **225**(2): p. 289-296.

57. Nielsen, T.H., L. Baunsgaard, and A. Blennow, *Intermediary glucan structures formed during starch granule biosynthesis are enriched in short side chains, a dynamic pulse labeling approach.* J Biol Chem, 2002. **277**(23): p. 20249-55.

58. Hussain, H., et al., *Three isoforms of isoamylase contribute different catalytic properties for the debranching of potato glucans.* Plant Cell, 2003. **15**(1): p. 133-49.

59. Streb, S., et al., *Starch granule biosynthesis in Arabidopsis is abolished by removal of all debranching enzymes but restored by the subsequent removal of an endoamylase.* Plant Cell, 2008. **20**(12): p. 3448-66.

60. Kim, D., S.K. Hwang, and T.W. Okita, *Subunit interactions specify the allosteric regulatory properties of the potato tuber ADP-glucose pyrophosphorylase.* Biochem Biophys Res Commun, 2007. **362**(2): p. 301-6.

VITA

Ayşe Bengisu Seferoğlu was born in Isparta, Turkey, on July 8, 1986. She received her B.Sc. Degree in Molecular Biology and Genetics from Istanbul Technical University, Istanbul, in 2009. From September 2009 to August 2011 she worked as teaching and research assistant at Koç University, Istanbul, Turkey. She has worked on "Identification of Important Residues for Modulation of Allosteric Properties of Potato ADP Glucose Pyrophosphorylase through Reverse Genetics" during her M.S. study.

Appendix A: Raw Data of the Sequences

Left side shows the sequence of the wild type, right side show the sequences of the random mutants

RM2

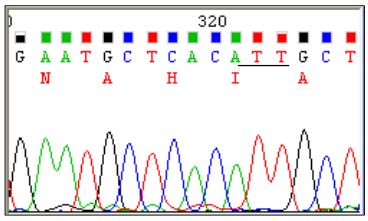

Ile 90

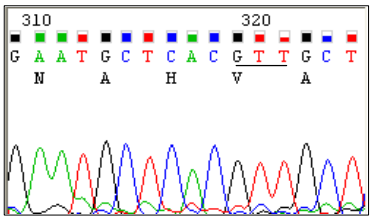

Val 90

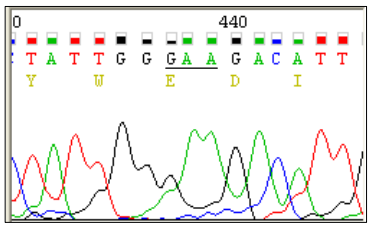

Glu 287

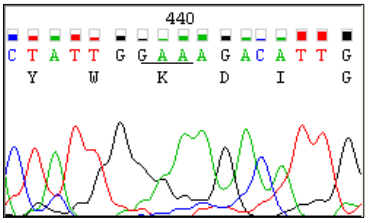

Lys 287

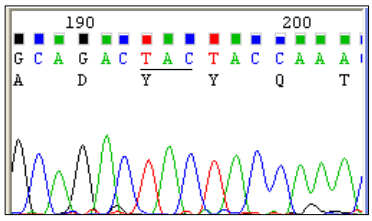

Tyr 378

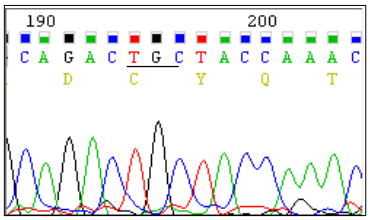

Cys 378

RM4

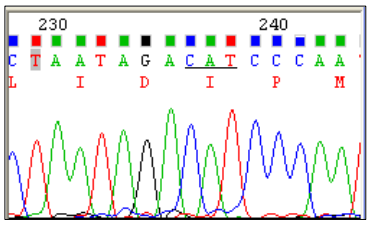

Ile 62

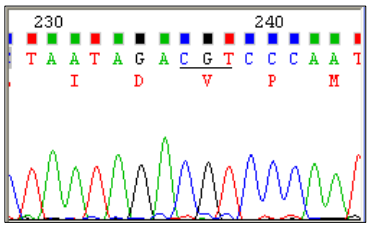

Val 62

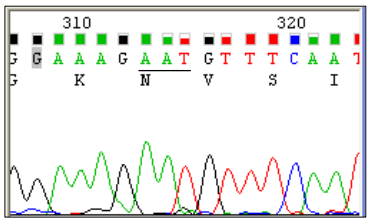

Asn 418

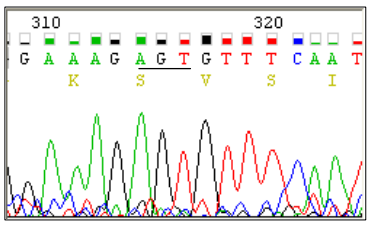

Ser 418

RM5

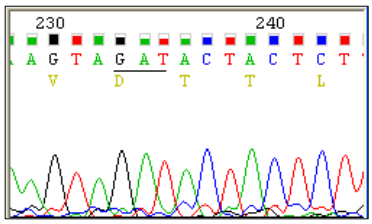

Asp 219

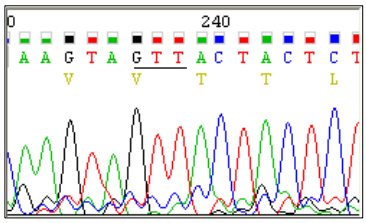

Val 219

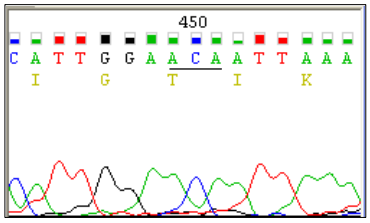

Thr 291

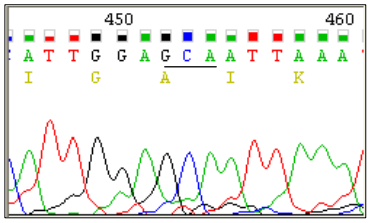

Ala 291

RM6

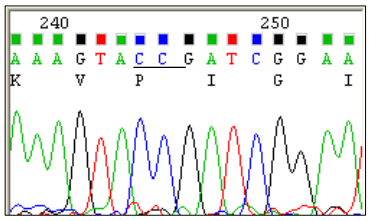

Pro 395

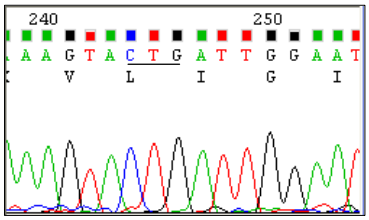

Leu 395

RM7

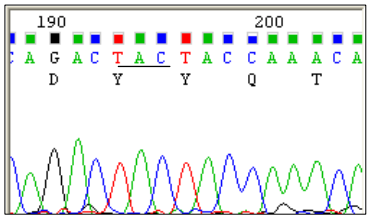

Tyr 378

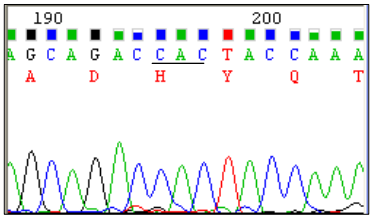

His 378

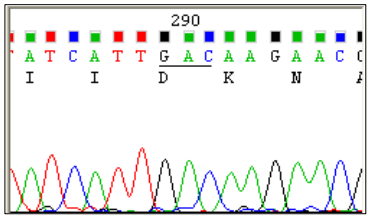

Asp 410

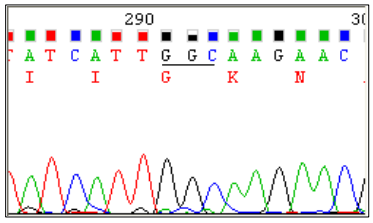

Gly 410

RM10

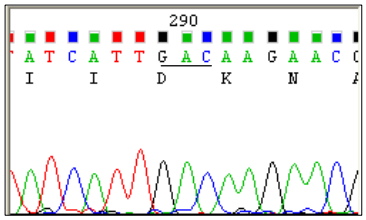

Asp 410

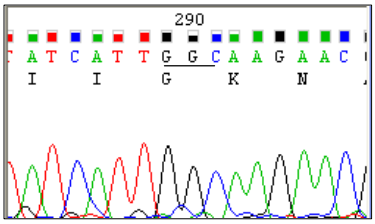

Gly 410

RM11

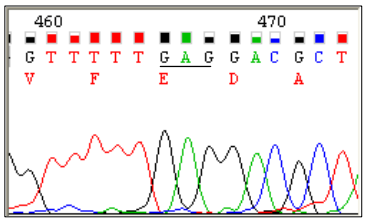

Glu 138

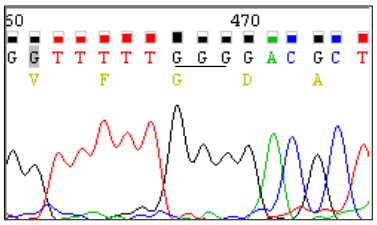

Gly 138

RM13

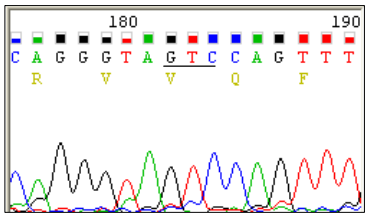

Val 202

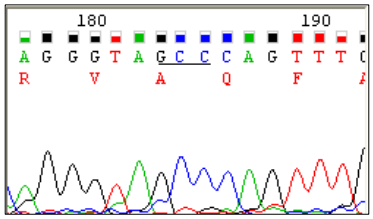

Ala 202

RM16

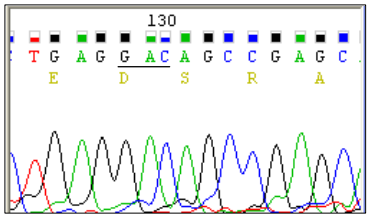

Asp 184

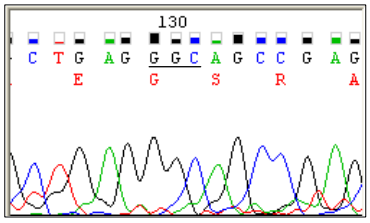

Gly 184

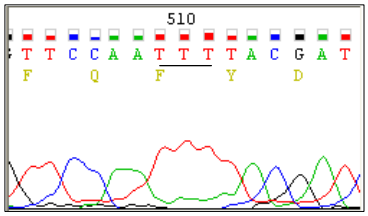

Phe 311

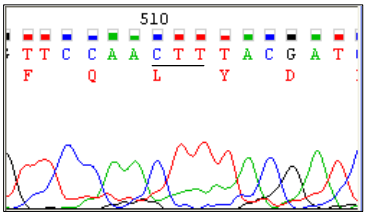

Leu 311

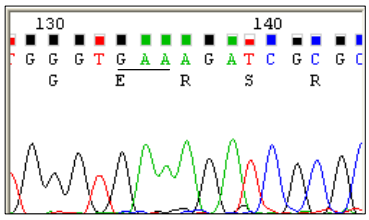

Glu 358

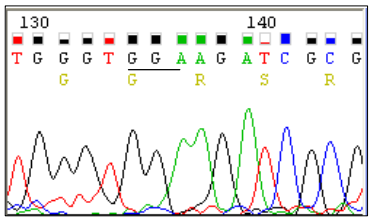

Gly 358

RM20

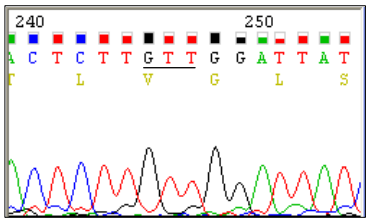

Val 223

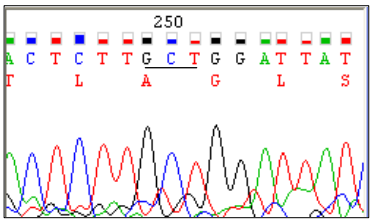

Ala 223

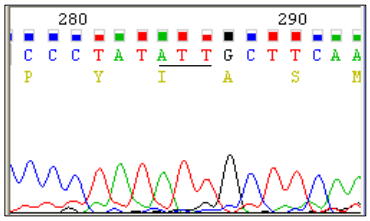

Ile 236

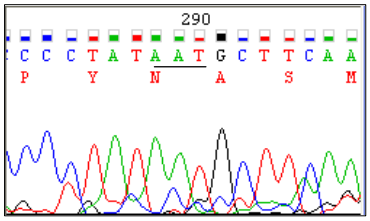

Asn 236

RM22

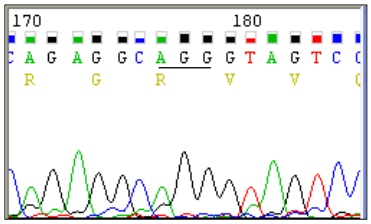

Arg 200

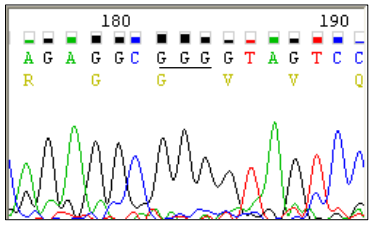

Gly 200

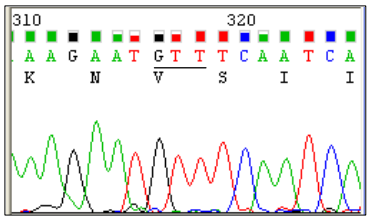

Val 419

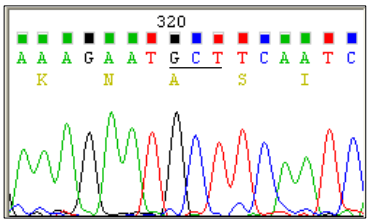

Ala 419

RM25

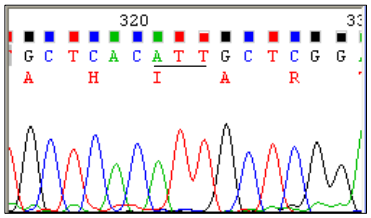

Ile 90

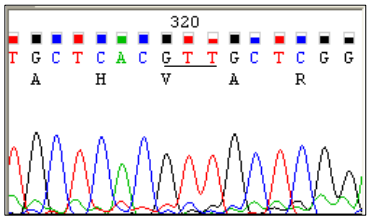

Val 90

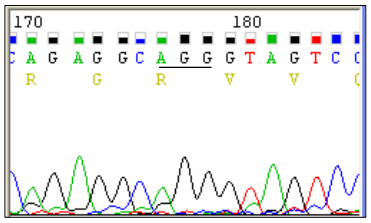

Arg 200

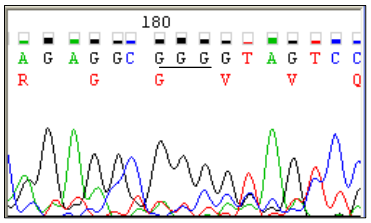

Gly 200

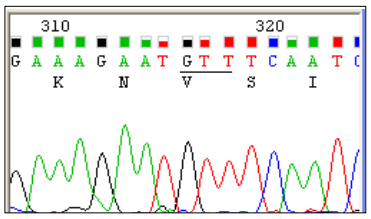

Val 419

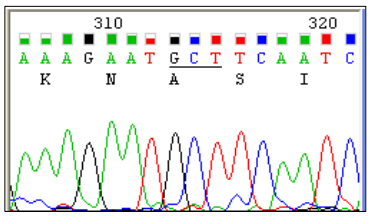

Ala 419

RM27

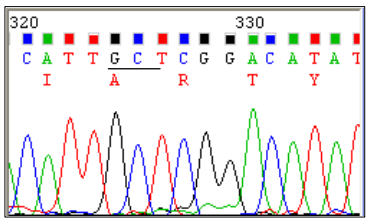

Ala 91

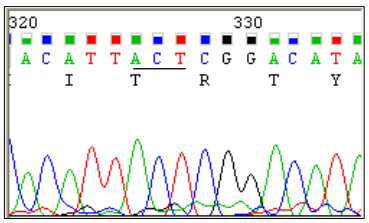

The 91

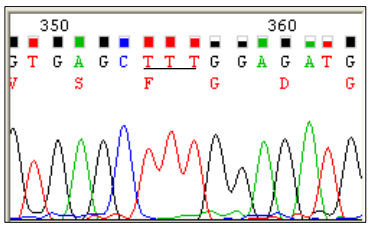

Phe 101

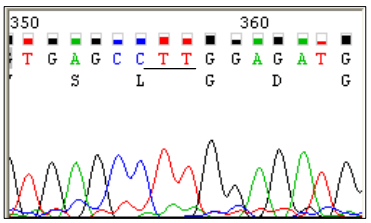

Leu 101

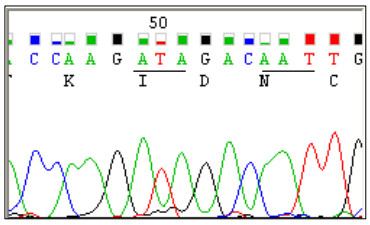

Ile 330
Asn 332

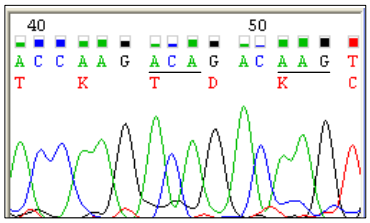

The 330
Lys 332

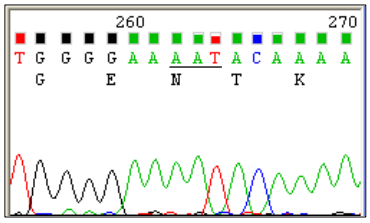

Asn 401

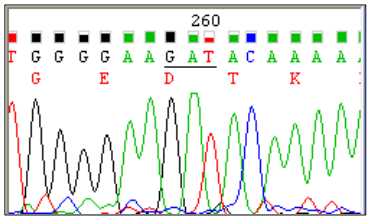

Asp 401

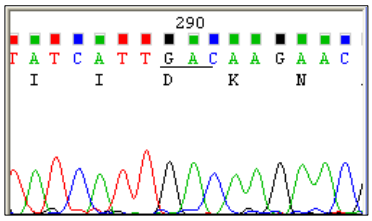

Asp 410

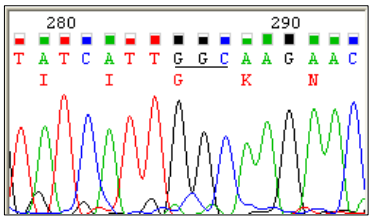

Gly 410

RM28

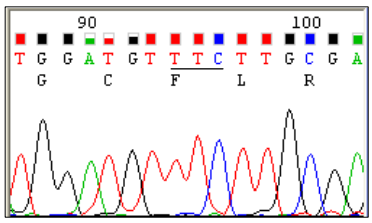

Phe 345

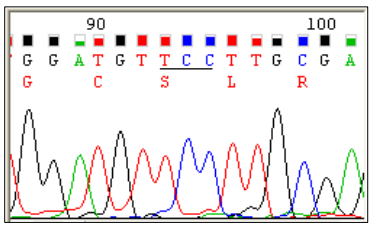

Ser 345

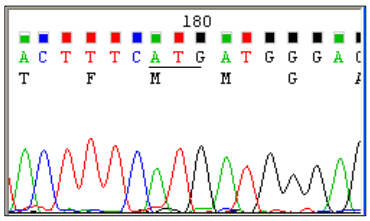

Met 373

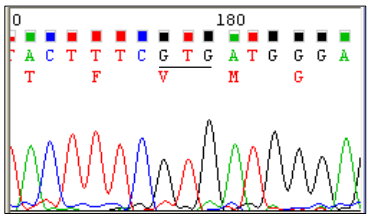

Val 373

Appendix B: Placement of Mutations on the Heterotetrameric Model

Placement of selected mutant residues (RM2, RM7, RM10, RM16 and RM27) on heterotetrameric model of the potato AGPase. Residues were indicated on the each snapshot. R88A residue is shown as black bonds and the other mutant residues are shown as colored balls.

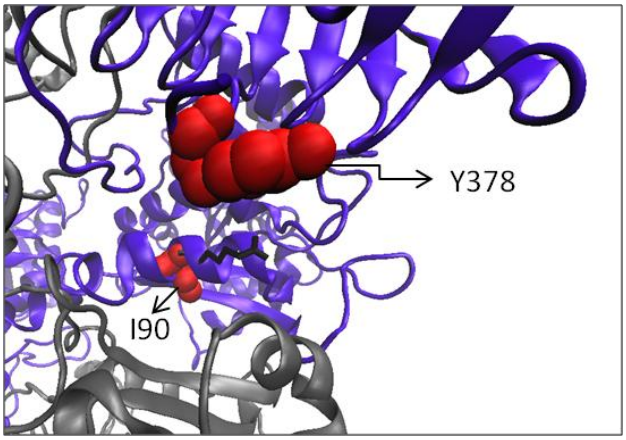

RM2

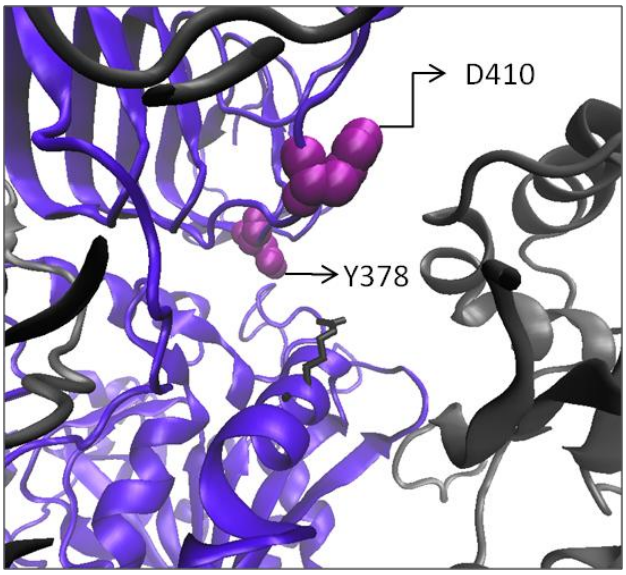

RM7

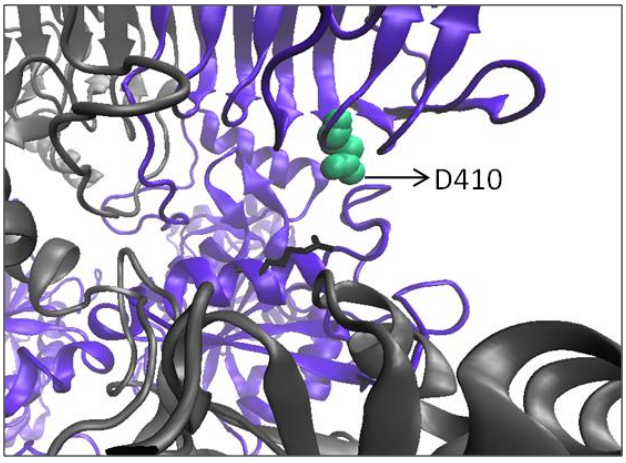

RM10

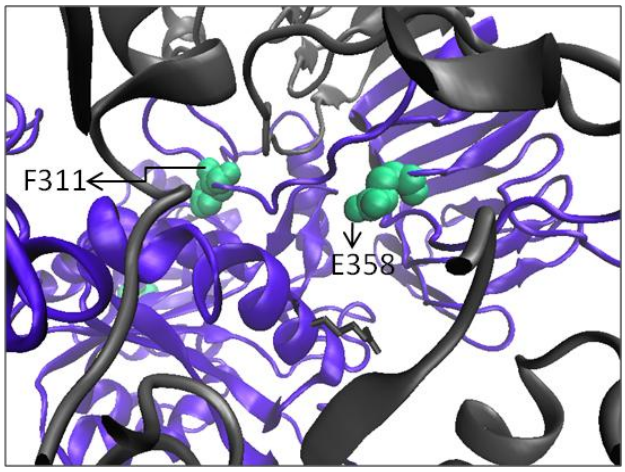

RM16

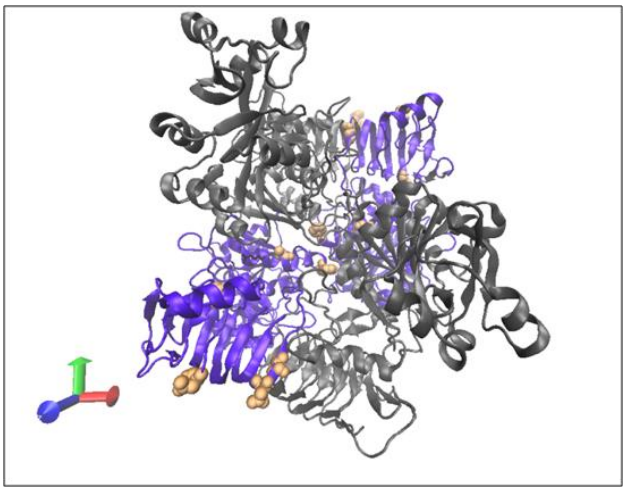

RM27

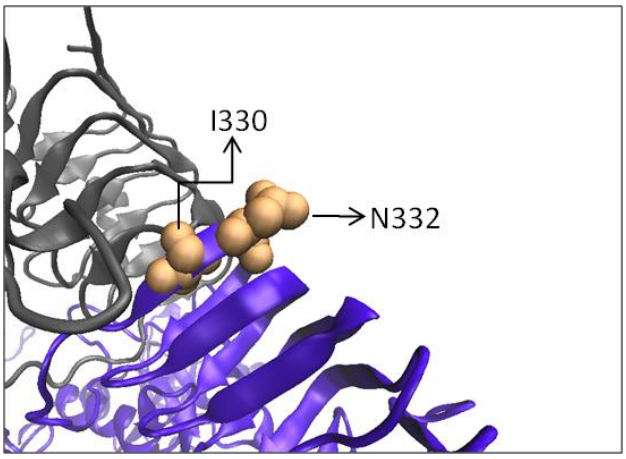

RM27

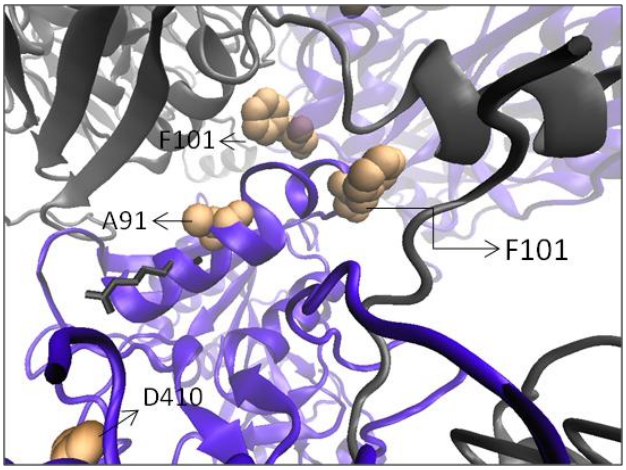

RM27

Appendix C: Kinetic Characterization Data

Graphs of the kinetic characterization data of wild type and mutant AGPases with substrates ATP and G1P and cofactor Mg^{2+} respectively.

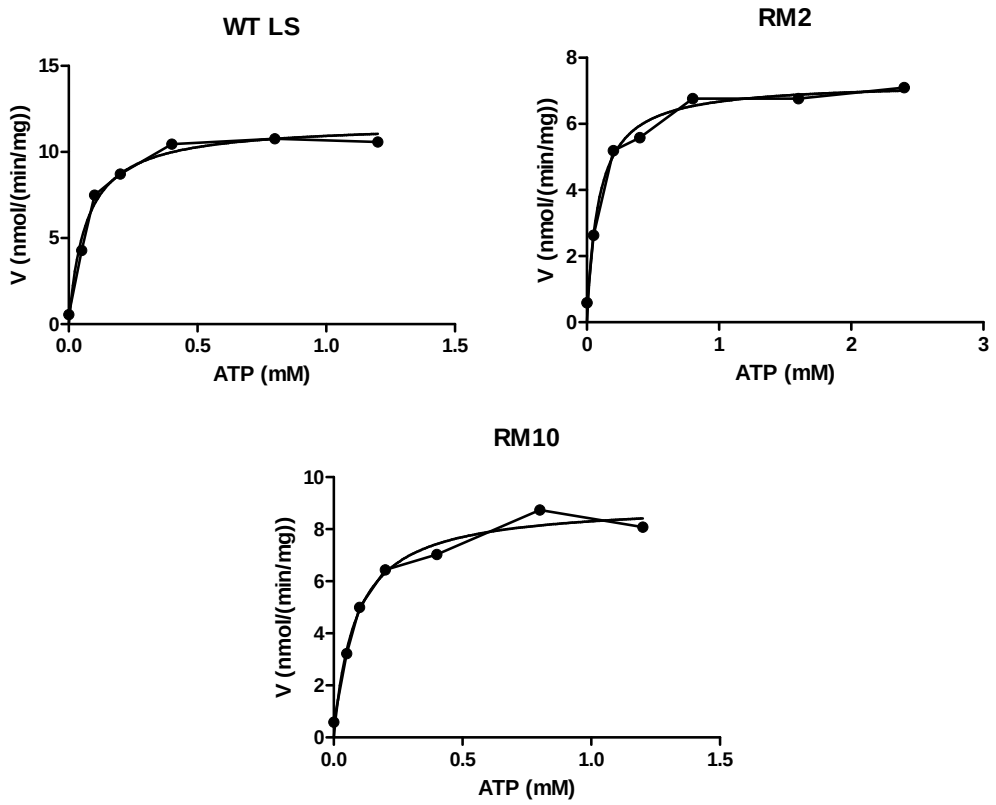

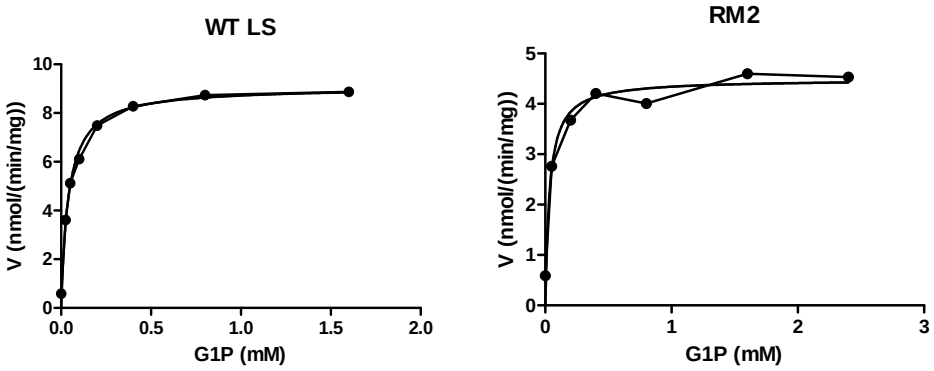
WT LS
V (nmol/(min/mg))
G1P (mM)
RM2
V (nmol/(min/mg))
G1P (mM)

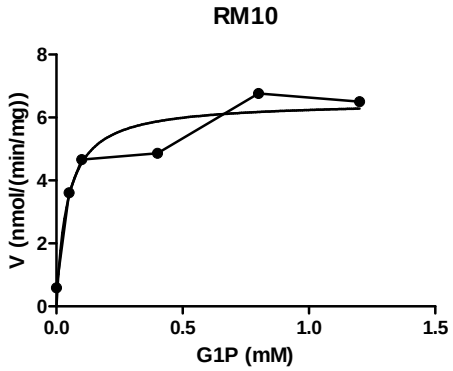
RM10
V (nmol/(min/mg))
G1P (mM)

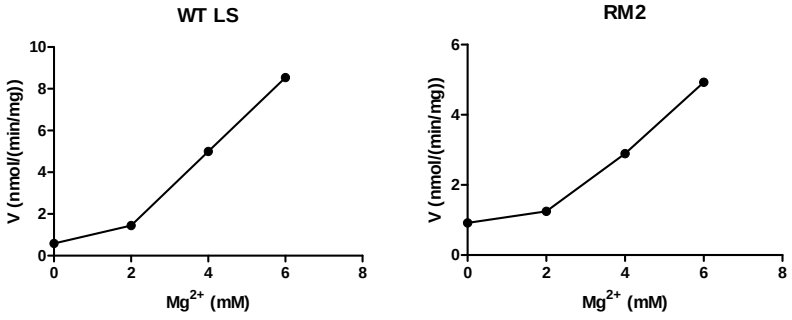
WT LS
V (nmol/(min/mg))
Mg2+ (mM)
RM2
V (nmol/(min/mg))
Mg2+ (mM)

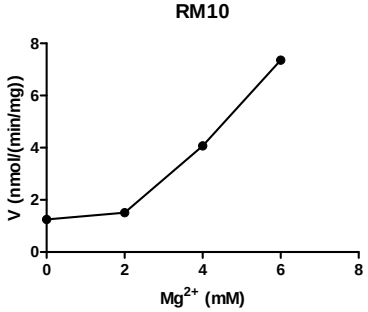
RM10
V (nmol/(min/mg))
Mg2+ (mM)

Appendix D: Map of Expression Vectors

LS expression vector pML7

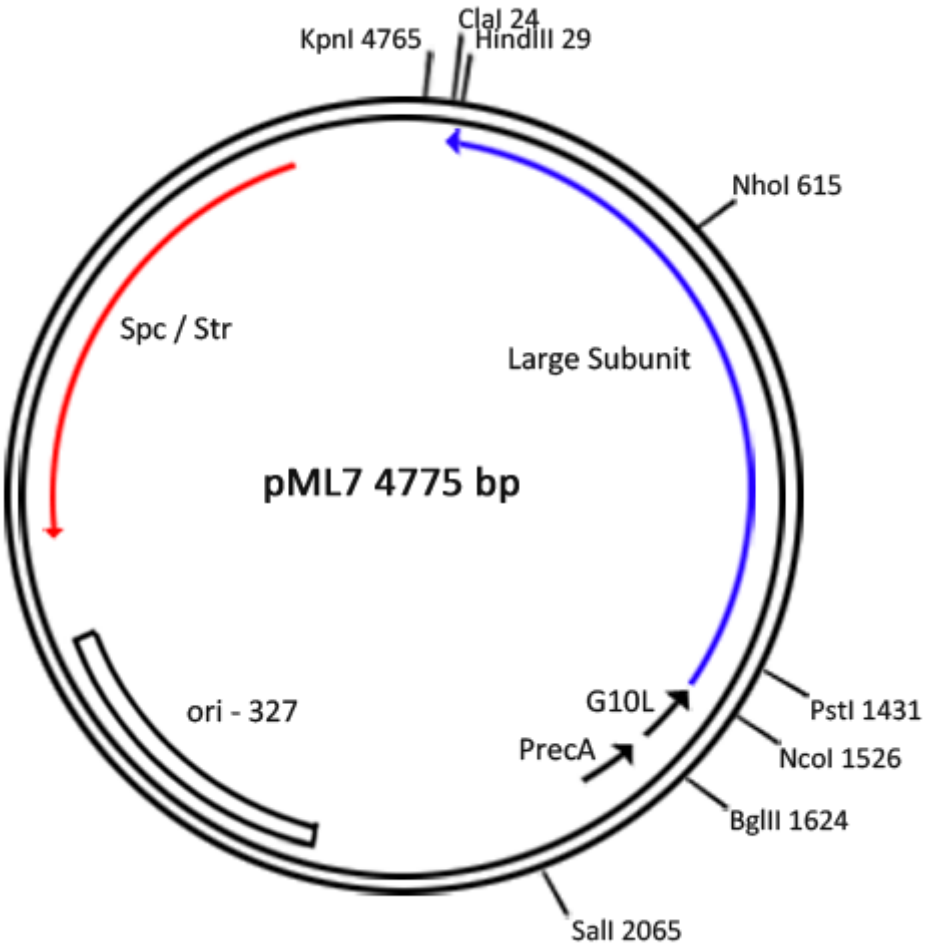

Appendix D: Map of Expression Vectors

SS expression vector pML10

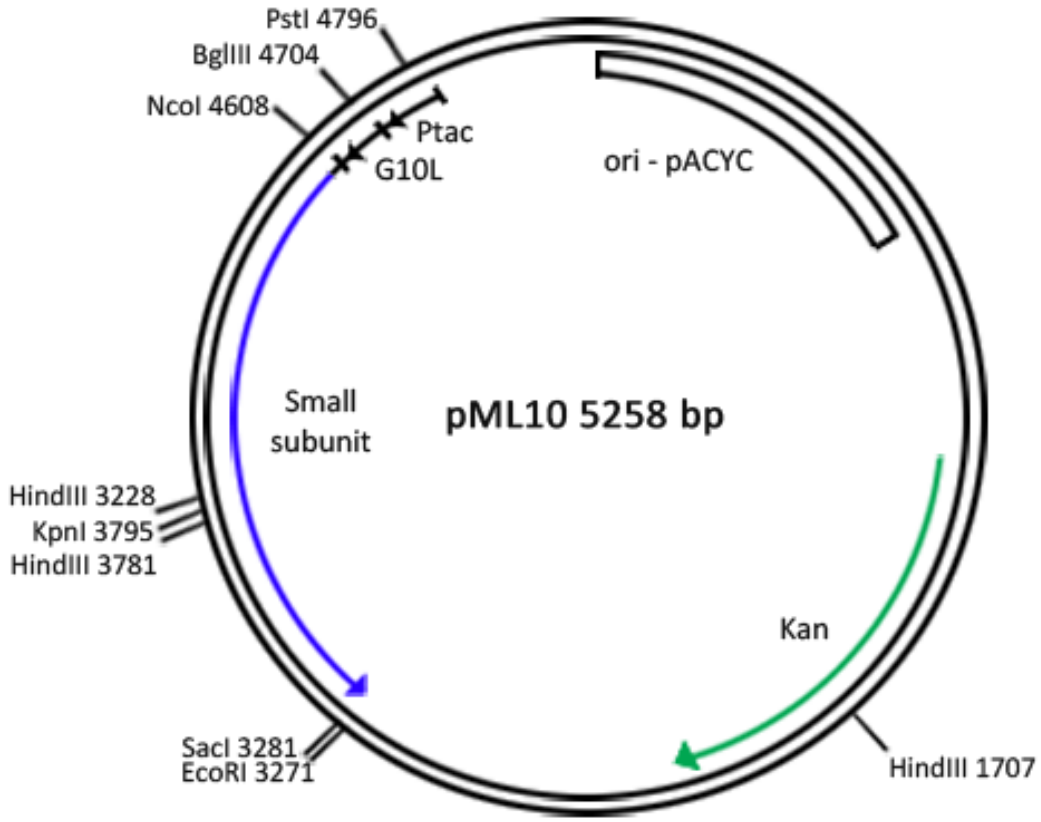

Appendix E: Primers

CLONING PRIMERS

LSDS1 5’-ACGTGCATCTTATCCATGGTGATCACTACTGAAAATGAC-3’

LSDS2 5’GAGGGCGCATAAGCTTTCATATGACTGTTCCATCTCTAATTG-3’

PRIMERS FOR SEQUENCING

1 5’-TAATACGACTCACTATAGGGC3’

2 5’-TCACACAAGAGTTTCCAGAG-3’

3 5’-GATGCTGTTAGAAAATTTATAGCGGTTTTTGAGGACGCTAAG-3’

SITE DIRECTED MUTAGENESIS PRIMERS

R88-F 5’-CTGCTCCCCTGAATCGTCACATTGCTCGAAC-3’

R 5’-GTTCGAGCAATGTGACGATTCAGGGGAGCAG-3’

RM2-F 5’-CTCCCCTGAATCGTCACGTTGCTCGAACATATTTT-3’

RM2-R 5’-CAAAATATGTTCGAGCAACGTGACGATTCAGGGGAG-3’

Appendix F: DNA and Protein Markers

DNA Molecular Weight Marker

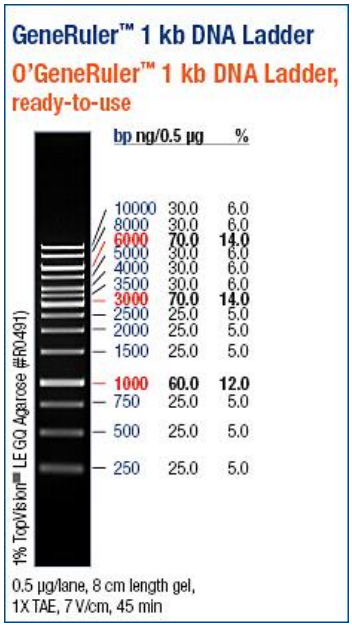

The ladder is a mixture of chromatography-purified individual DNA fragments.

Protein Molecular Weight Marker

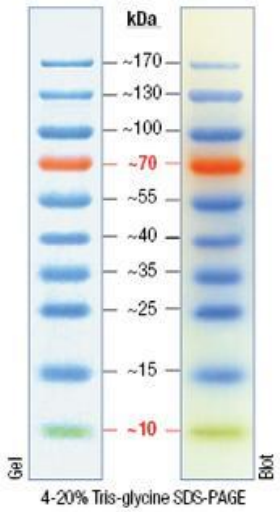

PageRuler Prestained Protein Ladders

Appendix G: Lab Equipments

Autoclaves	**:** CL-40S/SDP (60L) ALP autoclave
Centrifuges	**:** 4K15, Sigma Laboratory
	: Microfuge 14-15, Sigma Laboratory
Deep freezes and refrigerators	**:** Heto Polar Bear 4410 ultra freezer, JOUAN Nordic A/S, catalog# 003431.
	: 2021 D deep freezer, Arcelik.
	: 1061 M refrigerator, Arcelik.
Electrophoresis equipments	**:** E-C Mini Cell Primo EC320, E-C Apparatus.
	: Mini-PROTEAN 3 Cell and Single-Row AnyGel Stand, Catalog# 165-3321,Bio-Rad.
Gel documentation system	**:** UVIpro GAS7000, UVItec Limited.
Ice Machine	**:** AF 10, Scotsman.
Shaker	**:** Innova 4300 incubator shaker
Magnetic stirrer	**:** Heidolph MR 3001
Pipettes	**:** Pipetteman P10, P 100, P1000, Eppendorf
pH meter	**:** Inolab pH level 1, order# 1A10-1113,
Power supply	**:** PowerPac Basic (300V,400mA,75W) Biorad
Pure water systems	**:** DV25 PureLab Option ELGA
Spectrophotometer	**:** W-1700 PharmaSpec, Shimadzu Corporation.
Vortexing machine	**:** Reax Top, Heidolph2.2.